Communication

Observation of early ZIF-8 crystallization stages with X-ray absorption spectroscopy

Ana Guilherme Buzanich,[a] Anicó Kulow,[a] Anke Kabelitz,[a] Christian Grunewald,[a] Robert Seidel,[bc] Ander Chapartegui,[ad] Martin Radtke,[a] Uwe Reinholz,[a] and Franziska Emmerling,[ac] Sebastian Beyer[ef]*

[a] *Federal Institute for Materials Research and Testing (BAM), Richard-Willstätter-Str. 11, 12489 Berlin, Germany.*
[b] *Helmholtz-Zentrum Berlin für Materialien and Energie, Albert-Einstein-Strasse 15, 12489 Berlin, Germany.*
[c] *Department of Chemistry, Humboldt-Universität zu Berlin, Brook-Taylor-Str. 2, 12489 Berlin, Germany.*
[d] *School of Analytical Sciences Adlershof, Albert-Einstein-Straße 5, D-12489 Berlin, Germany*
[e] *Institute for Tissue Engineering and Regenerative Medicine, Chinese University of Hong Kong, Hong Kong SAR of China.*
[f] *Department of Biomedical Engineering, Chinese University of Hong Kong, Hong Kong SAR of China. Email: sebatsian.beyer@cuhk.edu.hk*

Contents

General Experimental procedure:

Zinc salt solutions were used at a concentration of 0.1 mol/l for three reasons. First, zinc salts are known to have the same octahedral mononuclear hexaquazinc^{2+} in aqueous solution only at concentrations lower than 0.2 mol/l while some zinc salts such as $ZnCl_2$ form more complex coordination compounds at higher concentrations[1]. Second, the relatively low concentration of metal ions allowed for a good x-ray transmission through the bulk medium of the liquid sample measurement cell. Third, this concentration regime allowed for sufficiently slow ZIF-8 crystallization to capture the mononuclear coordination species of interest. The zinc salt solution was loaded into the liquid sample measurement cell and placed into the dispersive XAS set-up. This methodology and related synchrotron hardware were designed and manufactured in-house by some of us[2]. 2-methylimidazole was used at a concentration of 0.8 molars aqueous solution. A 1:1 mixture of a double concentrated zinc salt solution and 2-methylimidazole solution was pumped rapidly through the flow cell to mimic the addition of 2-methylimidazole in a very defined concentration. After 10 s, the exchange with the mixture was stopped. During and after the exchange of the liquids, XAS spectra were continuously collected with a temporal resolution of 2 seconds. All reagents were obtained in reagent grade or higher quality from Sigma-Aldrich, Germany.

Tetrakis(1-methylimidazole)zinc(II)nitrate was obtained by mixing equal volumes of 0.2 mol/liter of zinc nitrate and 0.8 mol/liter 1-methylimidazole solutions to yield 0.1 mol/liter tetrakis(1-methylimidazole)zinc(II)nitrate prior to measurements.

[1] Structural characterization of zinc(II) chloride in aqueous solution and in the protic ionic liquid ethyl ammonium nitrate by xray absorption spectroscopy. Paola D'Angelo, Andrea Zitolo, Francesca Ceccacci, Ruggero Caminiti, and Giuliana Aquilanti. J. Chem. Phys. 135, 154509 (2011); https://doi.org/10.1063/1.3653939

[2] A new experimental setup for time- and laterally resolved X-ray absorption fine structure spectroscopy in a 'single shot'. A. Kulow, S. Witte, S. Beyer, A. Guilherme Buzanich, M. Radtke, U. Reinholz, H. Riesemeier and C. Streli. J. Anal. At. Spectrom., 2019, 34, 239, DOI: 10.1039/c8ja00313k.

DXAFS setup at the BAM*line* of the synchrotron facility BESSY II

The principle of the DXAFS setup at the BAMline differs from conventional DXAFS and QEXAFS setups at beamlines that are dedicated to time resolved XAS. As previously reported[3], there are two options to generate the incoming broadband beam are used, both using a Double Multilayer Monochromator (W/Si, with $\Delta E/E \cong 1.7\%$). The first option combines the DMM in total reflection ('mirror') mode with a filter to obtain an energy bandpass. This configuration allows a large usable energy range, which is necessary for EXFAS measurements. The second option is to use the intrinsic bandwidth of the DMM by setting it at the required energy. This covers in all cases the required XANES range. For the purpose of this work, we used the second option, setting the DMM at an energy of 9.7 keV, which results in a total of about 167 eV energy range.
The transmitted beam though the sample is dispersed by a convexly bent Si (111) crystal, allowing the different energies to be reflected under different angles and spatially separated in a single shot. An area sensitive detector records the reflected radiation – in this case a CCD-based camera with a Gd-based fluorescent screen were used. The CCD is a pco.4000 manufactured by PCO AG (Kelheim, Germany). It has a resolution of 4008 × 2672 pixels with a pixel size of 9 µm × 9 µm.
A scheme of the DXAFS setup is shown in Scheme 1. This setup is easy to install at the multipurpose beamline and can be fast adapted to different energies/experiments. Although faster time resolution is possible with this CCD camera, the used time-resolution is 1 s. This is not comparable to the time-resolution of dedicated DXAFS or QEXAFS beamlines, but enough for applications and case studies where dynamic processes occur on the second timescale.

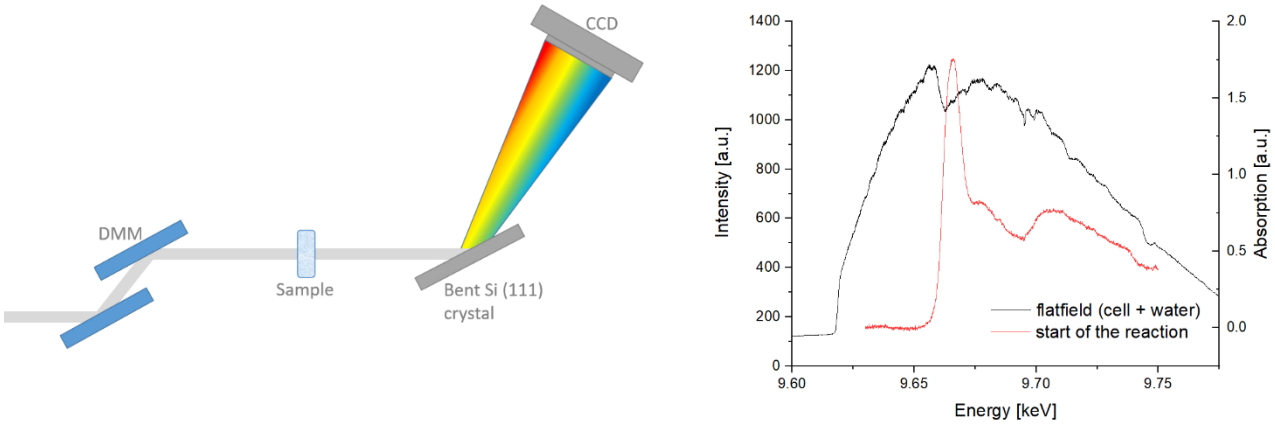

Scheme 1: a) scheme of the DXAFS setup at the BAMline. b) measurement of the flatfield (measurement cell filled with water) together with a spectrum from the start of the reaction

For the investigation of the ZIF-8 synthesis, and in order to remove energies below 5 keV, an 0.06 mm Aluminum filter was used. After every reaction, a measurement of the flatfield was recorded and subtracted to the images stored every second. In this case the flatfield consisted in the recorded intensity of the cell filled

[3] A new experimental setup for time- and laterally resolved X-ray absorption fine structure spectroscopy in a 'single shot'. A. Kulow, S. Witte, S. Beyer, A. Guilherme Buzanich, M. Radtke, U. Reinholz, H. Riesemeier and C. Streli. J. Anal. At. Spectrom., 2019, 34, 239, DOI: 10.1039/c8ja00313k.

with water at the same sample position with the same experimental parameters (Scheme 1, part b) The images were treated in ImageJ and exported as text files in order to be further analyzed in Athena[4]

The crystal had an angle θ = 11.18° relative to the incoming beam, that corresponds to an energy of 9.668 keV reflected in the middle of the crystal. The bending radius was approximately 1050 mm to ensure that all energies of interest could be detected on the CCD screen in a distance of 520 mm from the crystal. Further details on the geometric considerations are found in our earlier communication by A. Kulow et al.[3].

The standards used for the linear combination were measured with conventional XAFS at the µSpot beamline (BESSY-II). In this case the beam was monochromatized with a Si(111) double crystal monochromator and the whole XANES range was scanned stepwise with increased energy resolution (0.5 eV) around the main absorption edge. In the pre-edge range 10 eV steps were used and the post-edge region was scanned with 1.5 eV steps. The data were treated in Athena[4]

[4] ATHENA, ARTEMIS, HEPHAESTUS: data analysis for X-ray absorption spectroscopy using IFEFFIT" , B. Ravel and M. Newville, J. Synchrotron Rad. 12, pp 537--541 (2005).

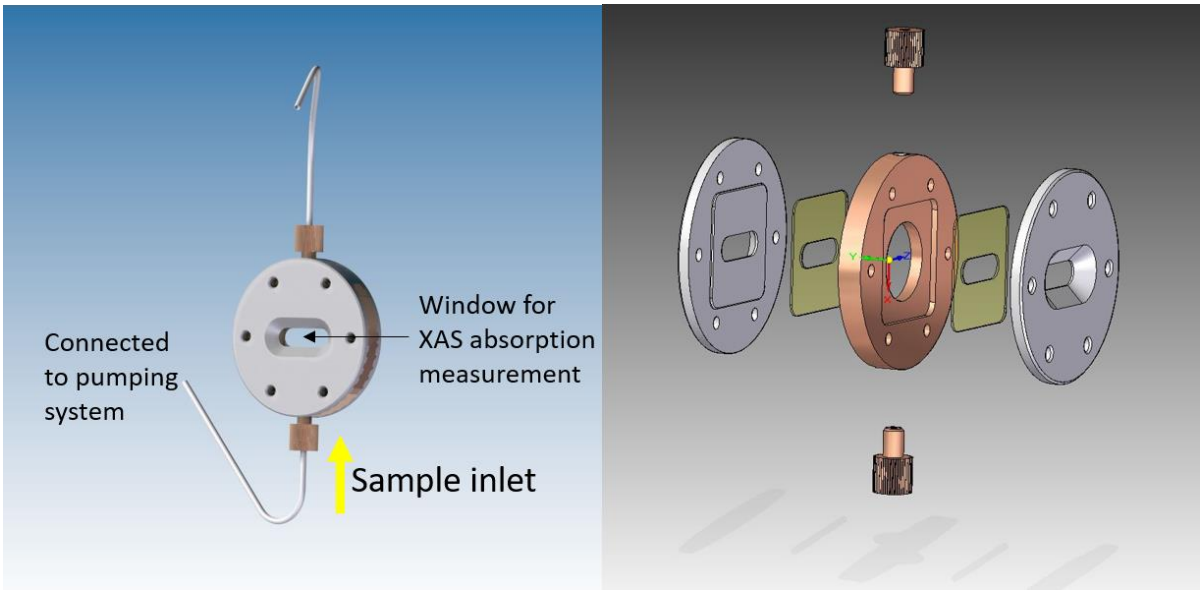

Figure S1: Liquid sample cell for in-situ XAS measurements.

The liquid sample measurement cell was designed and manufactured in the workshop of the Federals Institute for Materials Research and Testing (BAM). The cell was designed as a flow-through cell (left image) that can be connected to tubing that may be connected to a syringe pumping system. The liquid sample measurement cell comprises of a polyetheretherketone (PEEK) body and tubing ports (right image, copper coloured parts), sealing plates (right image, brass coloured parts) and casing (grey coloured parts) made of Acrylonitrile-butadiene-styrene co-polymer (ABS). An ultrathin quartz cover slide or thin Kapton foil was typically placed on each side between the body and the sealing plates. The assembled liquid sample measurement cell (including quartz slides or Kapton foil) was held together by 6 small metal screws. The technical drawings show that the total volume of the cell is much bigger than the window for x-ray transmission. Compared to a slit-shape, the cylindrical shape of the reaction reservoir within the liquid sample measurement cells causes a larger volume to be exchanged, while the windows withstand the pump pressure and keep their flat shape. Conserving the flat shape ensures that the liquid thickness doesn't vary during the measurements. Therefore, a cylindrical reservoir is advantageous for rapid convective mixing (less than 2 seconds) upon injection of a second solution.

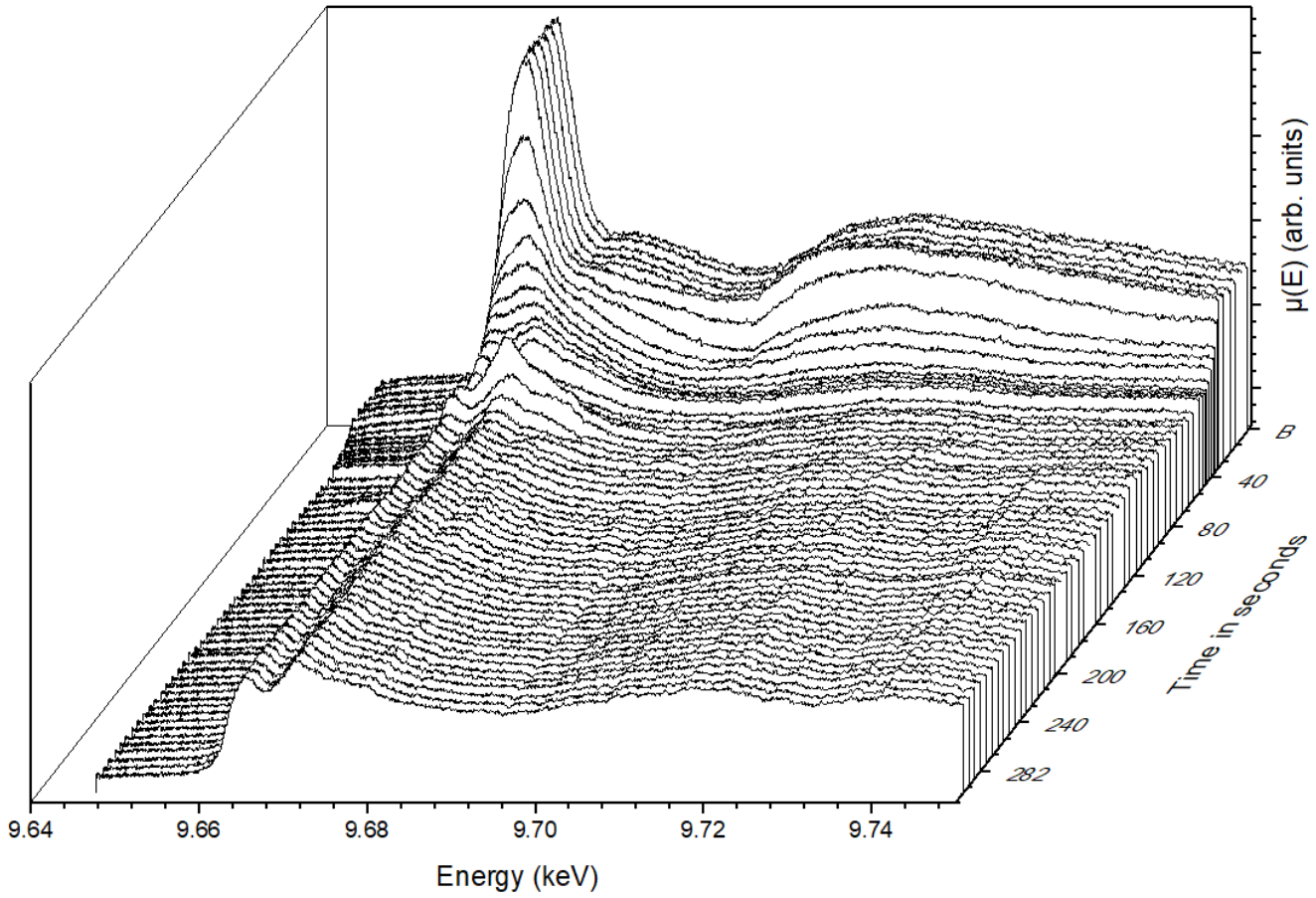

Figure S2: Full time-resolved XANES spectra during the first 300 seconds of ZIF-8 crystallization

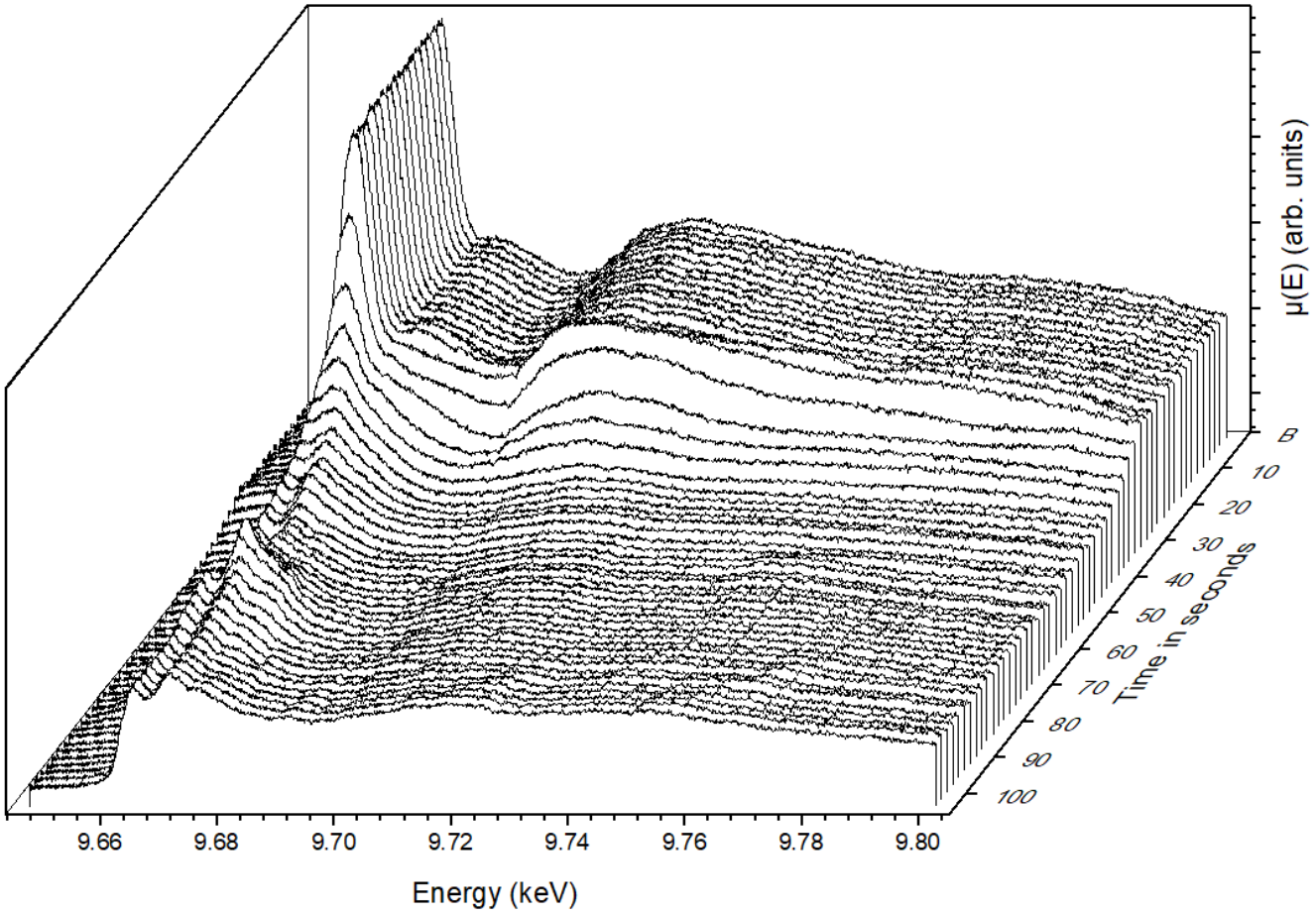

Figure S3: time-resolved XANES spectra during the first 120 seconds of ZIF-8 crystallization

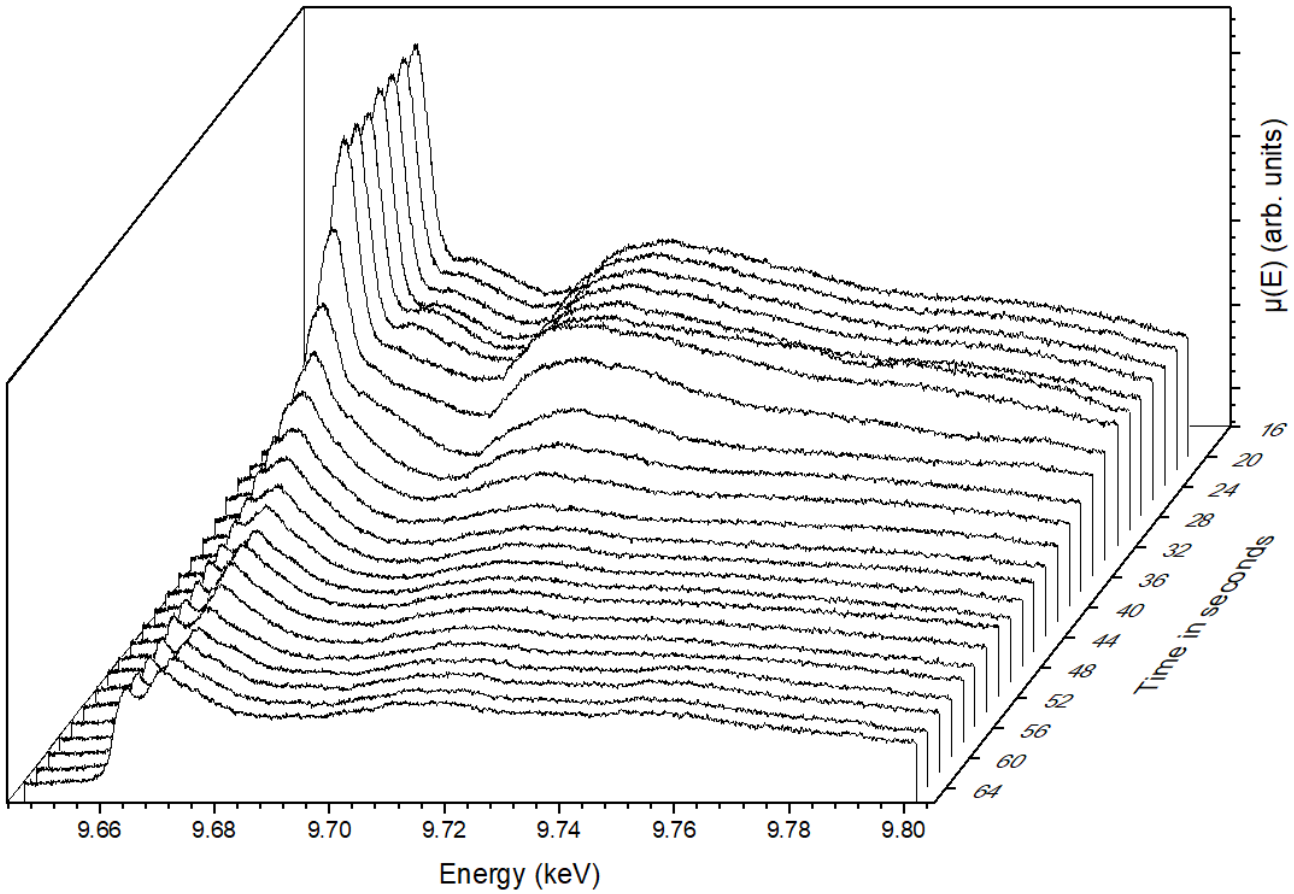

Figure S4: time-resolved XANES spectra during the first 70 seconds of ZIF-8 crystallization

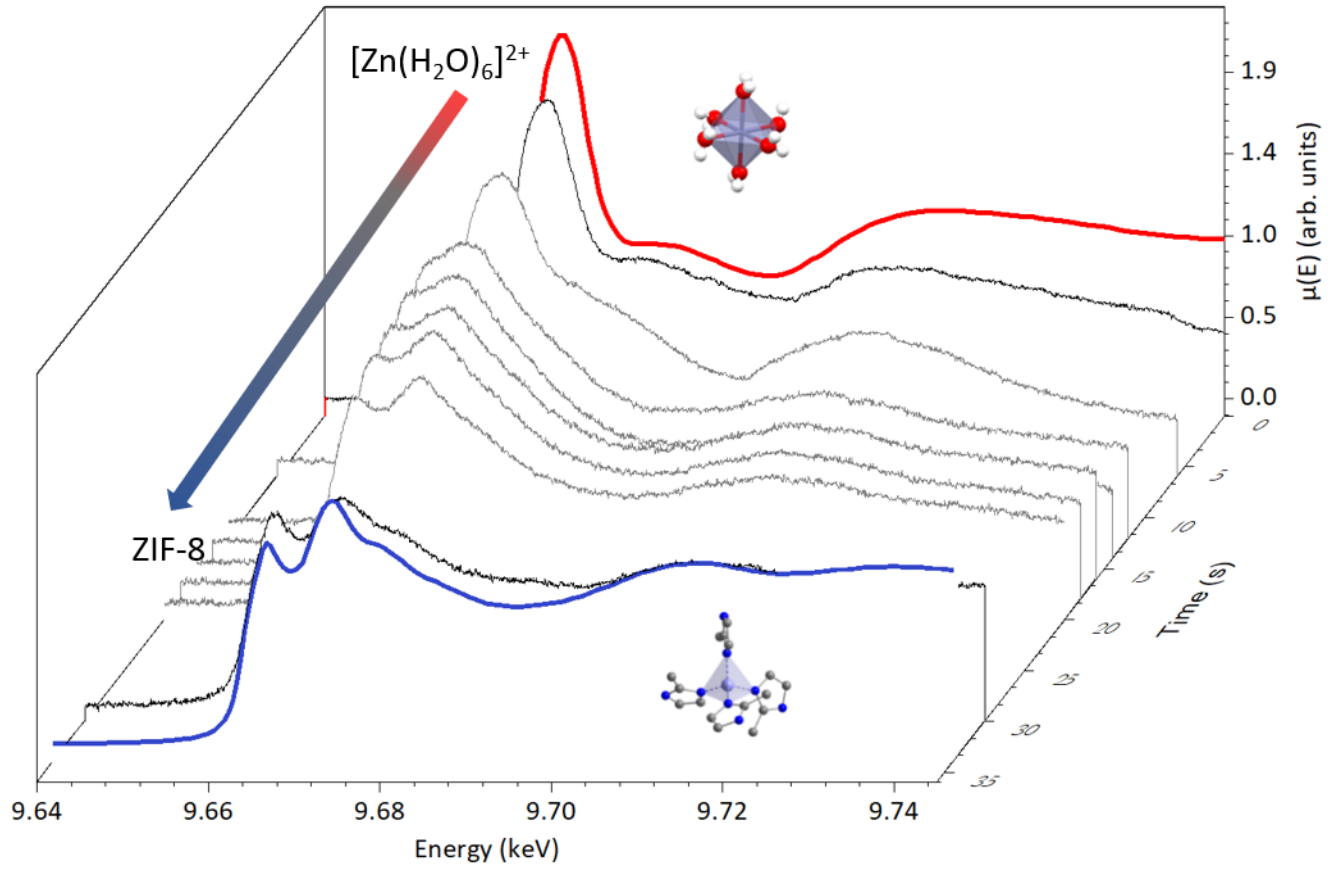

Figure S5: An overlay of time-laps XAS spectra (grey colour) and aqueous 0.1 molar zinc chloride solution (red colour) and solid ZIF-8 (blue colour).

Comparing the spectra of time-resolved measurements with static XAS of aqueous zinc nitrate and solid ZIF-8 clearly shows that XAS spectra has predominant features of ZIF-8 30 seconds after mixing. The presence of other species including unreacted mononuclear species cannot be excluded at any time-point however XAS indicates that the majority of zinc ions are bound into 2-methylimidazolate coordination tetraeder within 30 seconds of mixing. The time-laps spectra between 10 and 16 seconds after mixing clearly resemble that of tetrakis(1-methylimidazole)zinc(II) nitrate in Figure S3. This is apparent by the predominant spectral features that can be associated with tetrakis(1-methylimidazole)zinc(II) nitrate while some features of the hexaqua complex at early stages and of ZIF-8 towards later time points can be subliminal recognized.

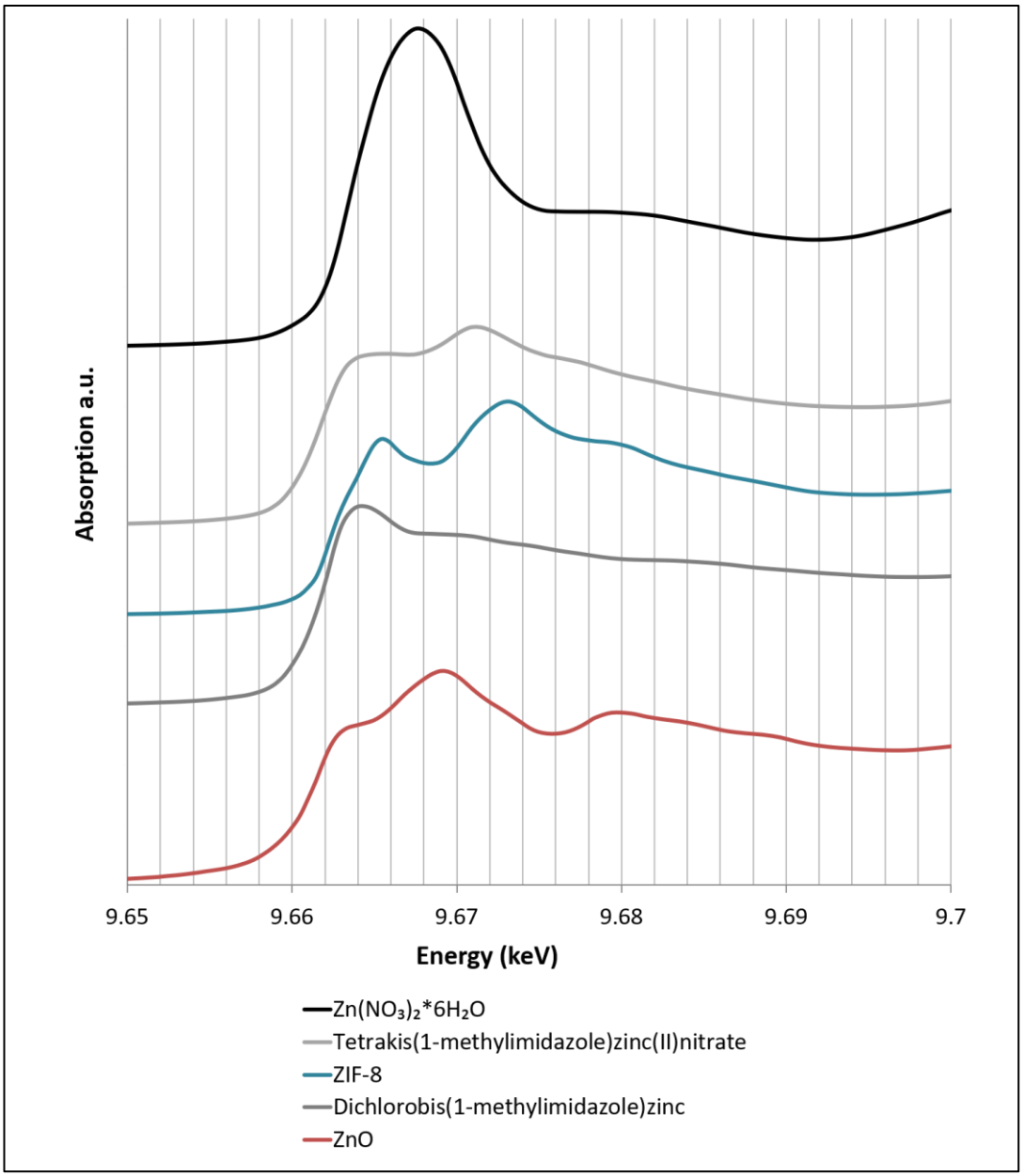

Figure S6: A detailed XAS comparison between the standards used for LCF.

Octahedral hexaquazinc(II)nitrate (black) was compared to tetrahedral coordinated zinc compounds from top to bottom; tetrakis(1-MeIM)zinc(II) nitrate (light grey), ZIF-8 (blue), dichlorobis(1MeIM)zinc(II) (grey) and zinc oxide (red).

Figure S2 shows significant differences between octahedral coordinated hexaquazinc(II)nitrate and tetrahedrally coordinated zinc components. The difference shows in the relative peak height as well as the peak width. The transition from the characteristic high and narrow peak for octahedrally coordinated Zn^{2+} towards the broader and lower peaks of tertrahedrally coordinated Zn^{2+} is as well visible in our recorded in-situ XAS, clearly showing the structural evolution from octahedral to tetrahedral coordination.

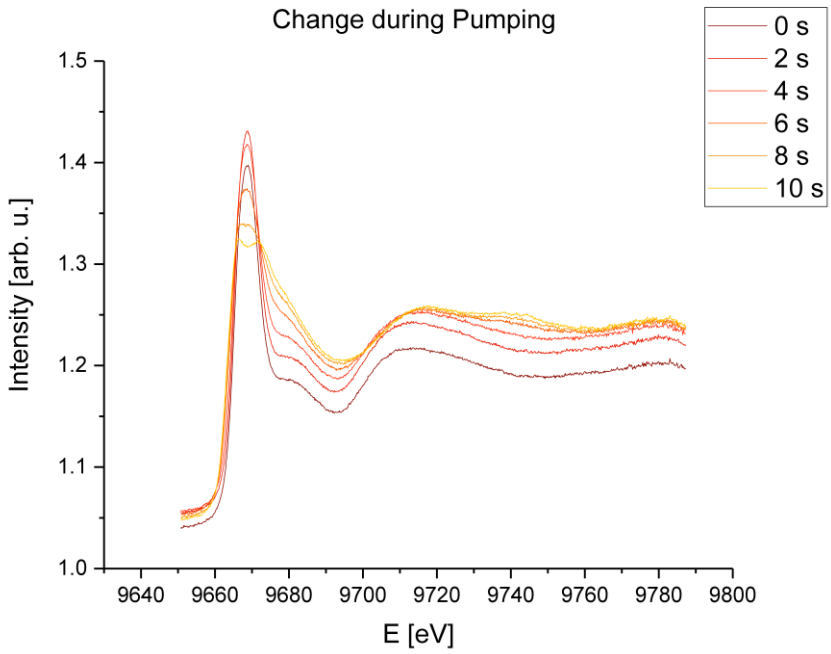

Figure S7: In-situ XAS kinetic of zinc acetate in presence of 2-methylimidazole (early)

The pumping of 2-methylimidazolate into the zinc acetate solution lasted 5-6 seconds, the first spectra (0 seconds) shows pure zinc acetate solution at 0.1 mol/l.

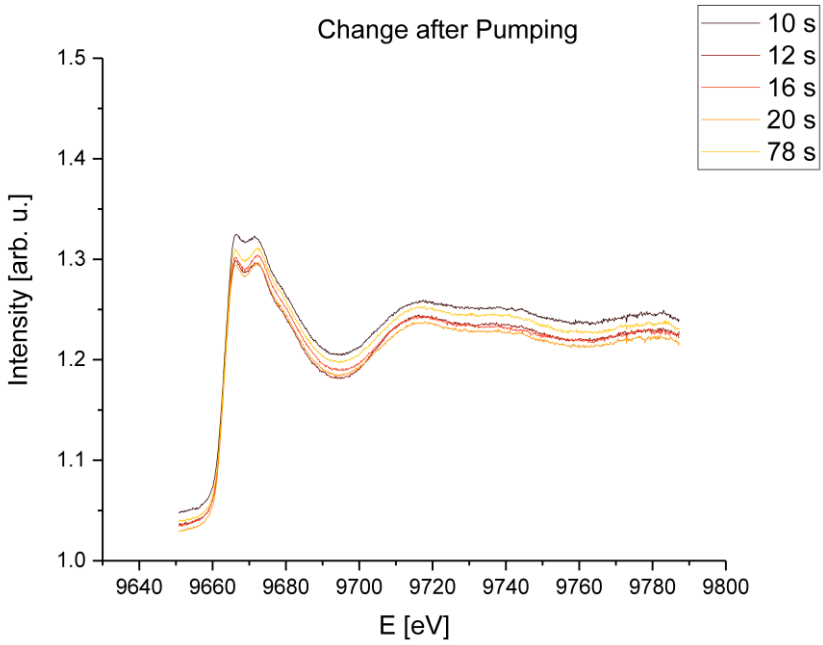

Figure S8: In-situ XAS of zinc acetate in presence of 2-methylimidazole (intermediate)

Later time points after pumping 2-methylimidazolate into the zinc acetate solution showed attenuation of ZIF-8 related features in XAS spectra, in particular relating to the formation of two local absorption maxima that is characteristic for ZIF-8 but not tetrakis(1-MeIM)Zn^{2+}.

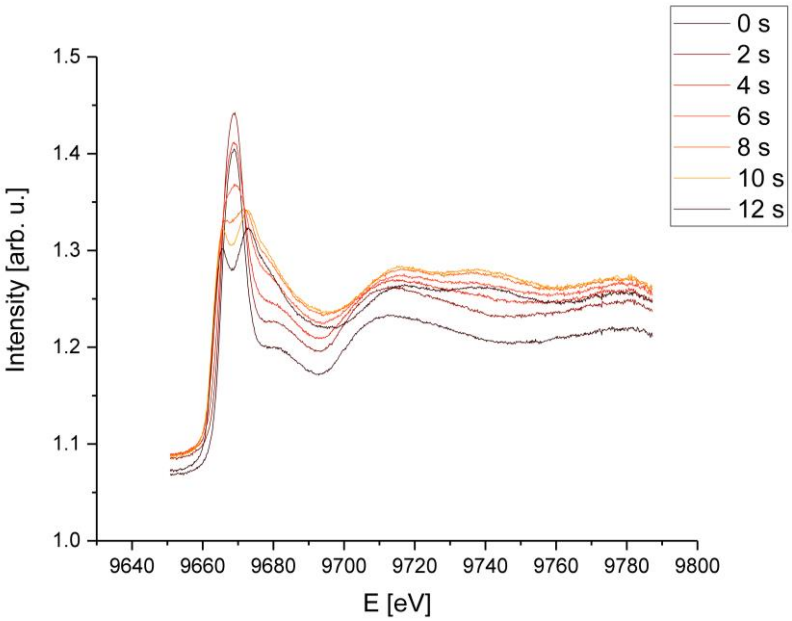

Figure S9: In-situ XAS on zinc chloride in presence of 2-methylimidazole (early)

The pumping of 2-methylimidazolate into the zinc chloride solution lasted 5-6 seconds, the first spectra (0 seconds) shows pure zinc chloride solution at 0.1 mol/l.

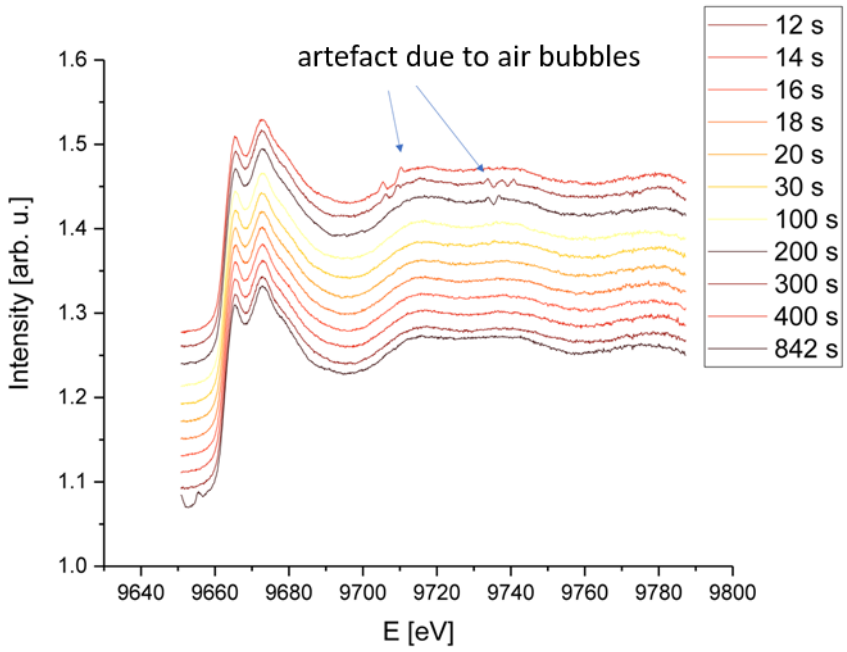

Figure S10: In-situ XAS of zinc chloride in presence of 2-methylimidazole (intermediate to very late)

No significant change in XAS could be observed for extended period of times, indicating no change in XAS spectra during crystal growth period of ZIF-8.

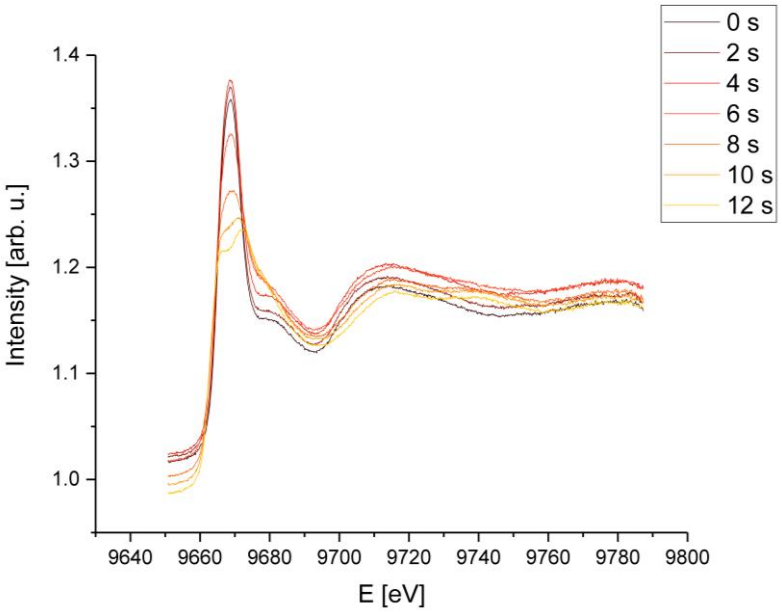

Figure S11: In-situ XAS of zinc nitrate in presence of 2-methylimidazole (early)

Structural transition of zinc nitrate in presence of 2-methylimidazole appears to proceed slightly slower compared to zinc acetate and zinc chloride, yet similar structural transitions can be observed.

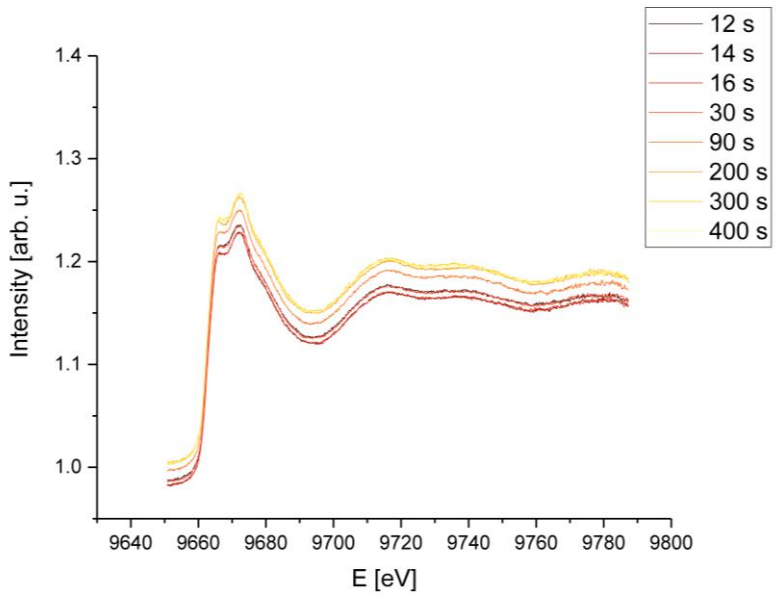

Figure S12: In-situ XAS of zinc nitrate in presence of 2-methylimidazole (late)

Similar to observations for other zinc salts, structural transition of zinc nitrate in presence of 2-methylimidazole occurs rather fast and only minor changes are observed during crystal growth in the crystallization process of ZIf-8.

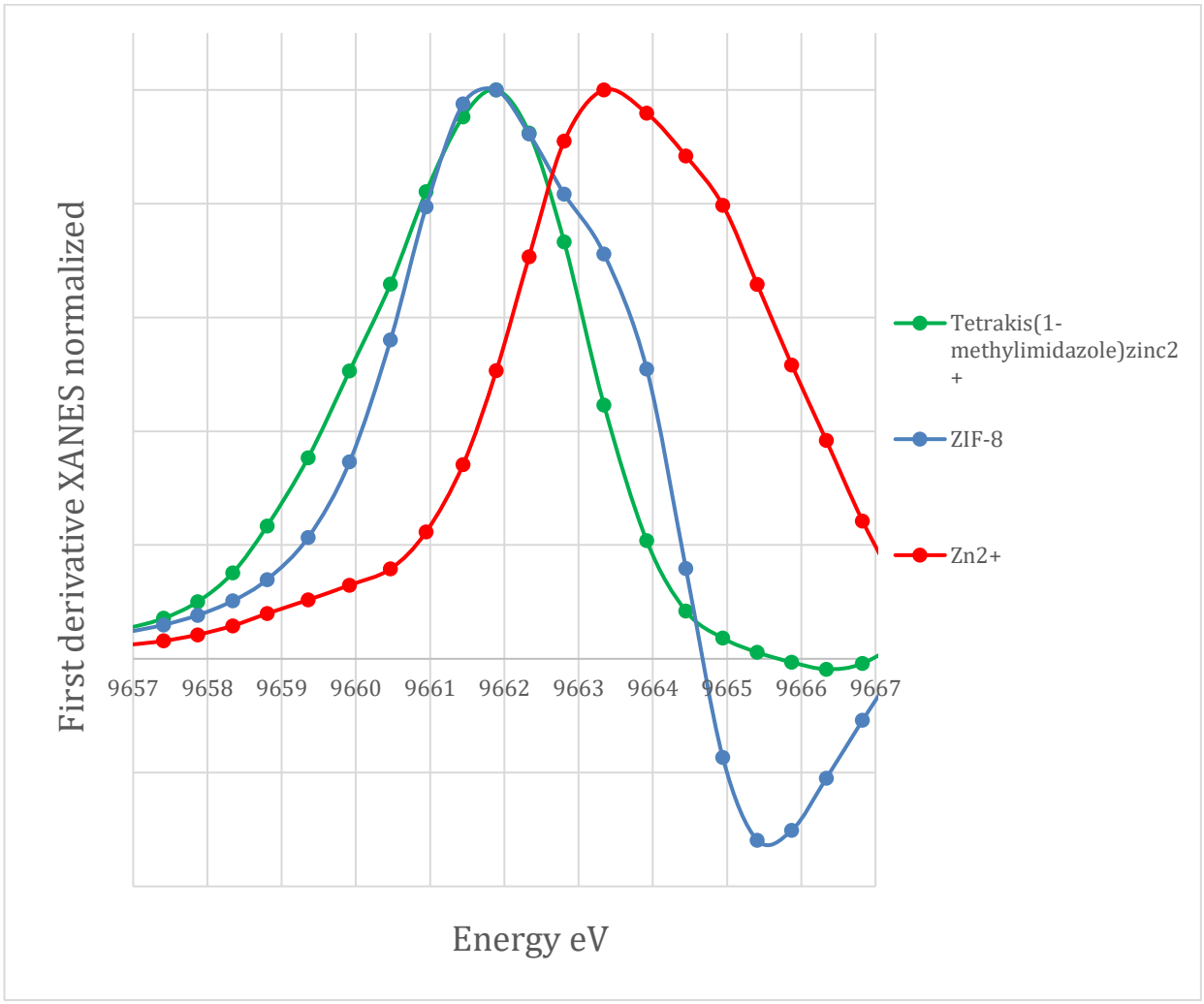

Figure S13: First derivative of XANES from standards for LCF, normalized to their maximum.

Seconds	hexaquaZn2+	Tetrakis(1-MeIM)	ZIF-8	Diclorobis(1-MeIM)	ZnO	Other	Sum
2	0.713627	1.42E-07	0.04537	1.05E-06	0.030845	0.210158	0.789842
4	0.730358	3.41E-09	2.68E-09	5.82E-08	4.91E-10	0.269642	0.730358
6	0.708817	6.72E-08	1.99E-06	6.38E-08	4.75E-05	0.291134	0.708866
8	0.70882	2.72E-08	9.54E-09	4.7E-08	4.59E-05	0.291134	0.708866
10	0.70882	2.72E-08	9.54E-09	4.7E-08	4.59E-05	0.291134	0.708866
12	0.722495	1.99E-08	2.68E-08	3.78E-08	2.38E-08	0.277504	0.722496
14	0.568433	7.12E-07	6.38E-07	0.206309	0.009463	0.215793	0.784207
16	0.571076	3.66E-08	3.9E-08	0.208273	0.002289	0.218362	0.781638
18	0.700817	1.49E-07	2.82E-07	2.54E-07	0.026136	0.273046	0.726954
20	0.689814	3.78E-08	1.16E-08	2.47E-08	0.040147	0.270038	0.729962
22	0.696362	1.92E-06	9.68E-06	8.29E-06	0.034061	0.269557	0.730443
24	0.562393	7.36E-07	2.79E-08	0.209435	0.010355	0.217815	0.782185
26	0.574165	1.83E-08	4.64E-08	0.210598	1.78E-08	0.215236	0.784764
28	0.588615	8.18E-08	0.054057	0.141597	6.18E-09	0.215731	0.784269
30	0.727021	9.16E-09	0.116647	1.03E-08	0.043166	0.113166	0.886834
32	0.683666	5.6E-08	0.066506	4.18E-08	6.58E-09	0.249828	0.750172
34	0.570076	0.022635	0.186901	6.23E-06	1.25E-05	0.220369	0.779631
36	0.557477	0.083581	0.301222	2.35E-08	1.36E-08	0.05772	0.94228
38	0.461918	0.149236	0.350252	1.06E-08	1.57E-08	0.038593	0.961407
40	0.465358	0.150358	0.391195	1.43E-08	5.89E-08	0	1.006911
42	0.441474	0.176465	0.475819	1.89E-08	4.51E-08	0	1.093757
44	0.362495	0.215097	0.389303	0.12719	4.66E-08	0	1.094085
46	0.289476	0.224916	0.41724	0.132945	1.03E-05	0	1.064586
48	0.264797	0.187607	0.581504	3.03E-07	1.34E-11	0	1.033908
50	0.160774	0.223771	0.460308	0.134181	3.51E-05	0.020931	0.979069
52	0.178575	0.191236	0.609223	0.010495	4.34E-06	0.010468	0.989532
54	0.157257	0.198197	0.621121	9E-05	7.19E-07	0.023335	0.976665
56	0.112979	0.234014	0.496177	0.128866	0.000193	0.02777	0.97223
58	0.13486	0.222994	0.423095	0.18856	4.47E-06	0.030487	0.969513
60	0.0694	0.219172	0.464239	0.167987	3.44E-06	0.079198	0.920802
80	0.095709	0.220161	0.617473	6.12E-05	9.42E-09	0.066596	0.933404
100	0.027147	0.340466	0.404273	0.000275	0.038417	0.189422	0.810578
120	0.030483	0.356831	0.421124	0.000285	5.33E-09	0.191277	0.808723
140	0.022519	0.362801	0.424654	0.00021	1.24E-08	0.189816	0.810184
160	0.018129	0.364257	0.424776	0.000213	2.3E-07	0.192625	0.807375
180	0.038309	0.36222	0.41918	0.000168	2E-08	0.180123	0.819877
200	0.041236	0.351258	0.406233	0.00028	2.66E-08	0.200992	0.799008
220	0.029635	0.38093	0.390065	0.000202	3E-05	0.199137	0.800863
240	0.121436	0.479313	0.508192	0.000179	3.11E-08	-0.10912	1.10912
260	0.011224	0.364308	0.409066	0.016793	0.005071	0.193538	0.806462
280	0.009845	0.359127	0.412688	0.023738	0.000437	0.194164	0.805836
300	0.014332	0.359684	0.417833	0.01131	8.83E-06	0.196833	0.803167

Table S1: numerical values plotted in figure 4 within the main text.

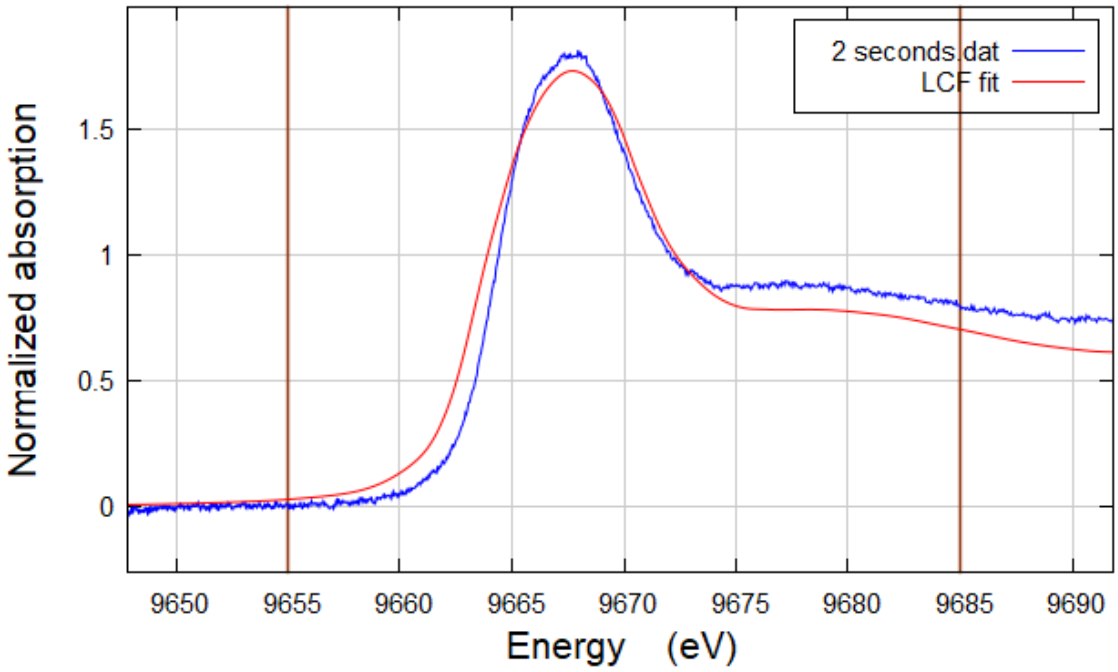

Figure S141: LCF of spectrum at 2 seconds

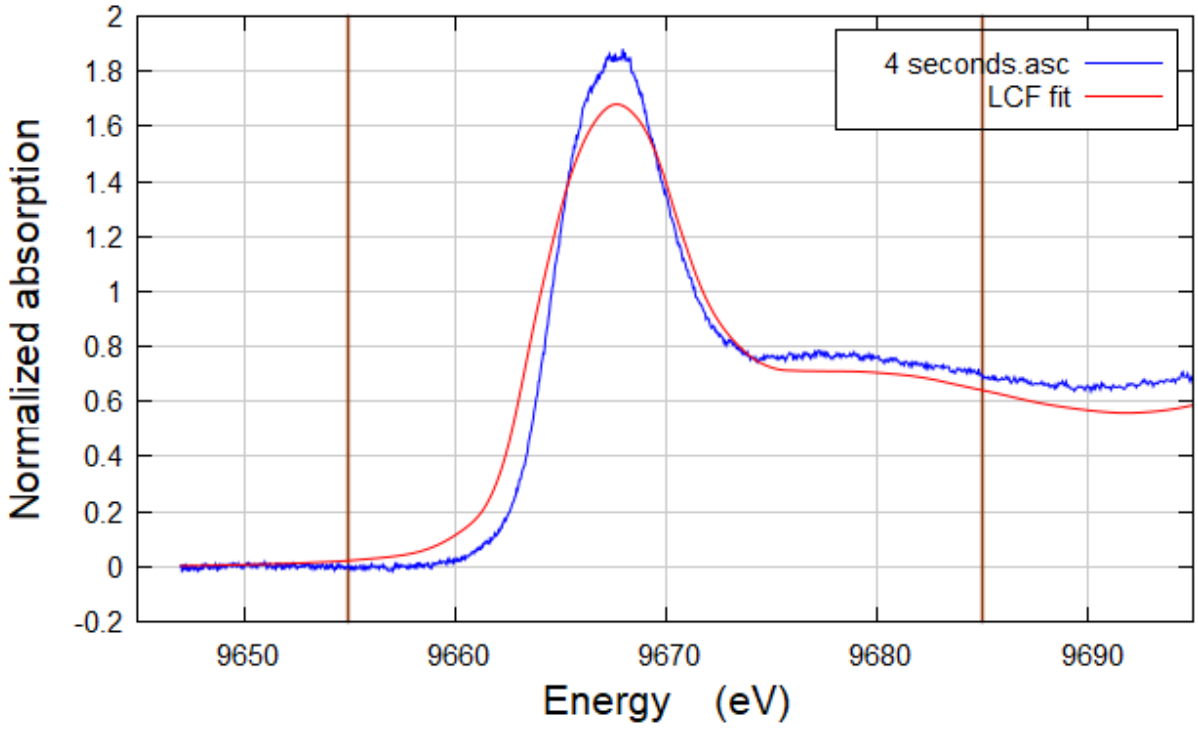

Figure S15: LCF of spectrum at 4 seconds

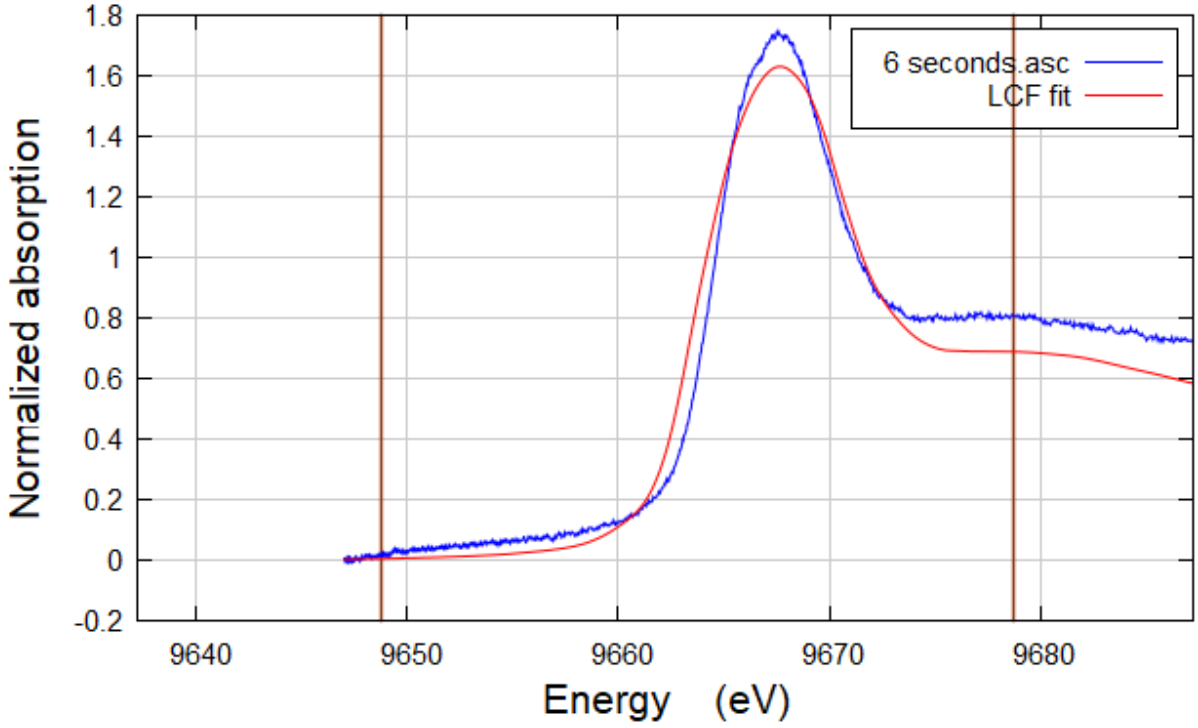

Figure S16: LCF of spectrum at 6 seconds

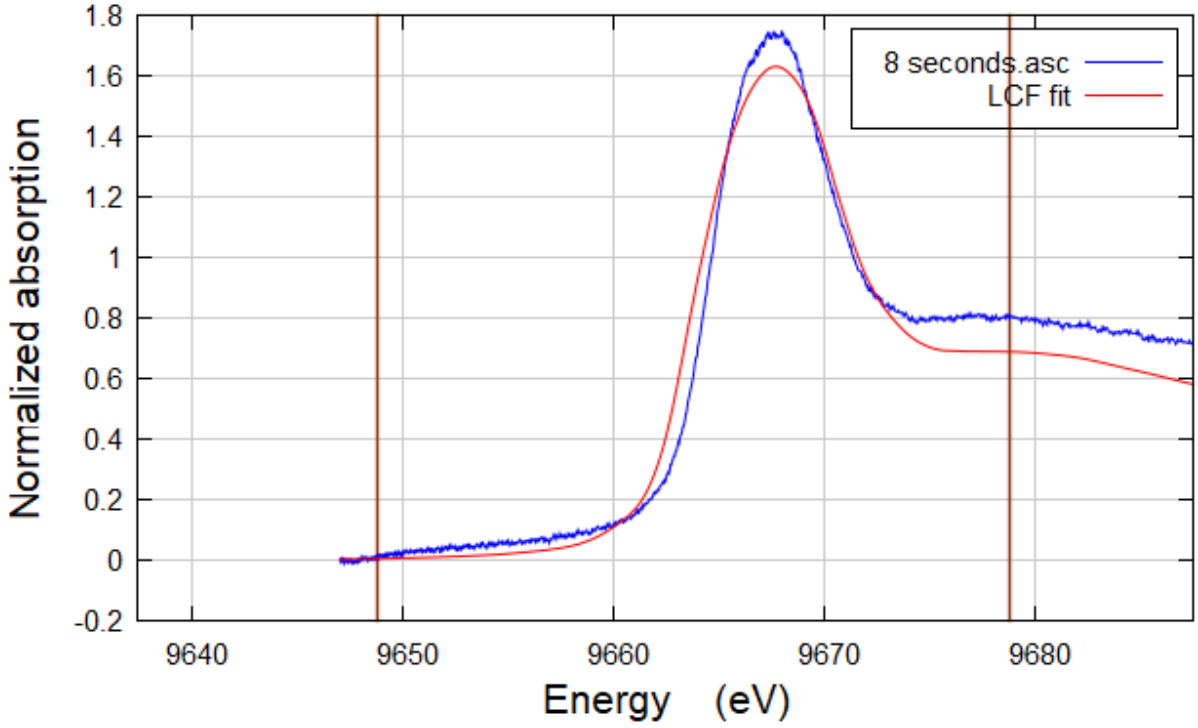

Figure S17: LCF of spectrum at 8 seconds

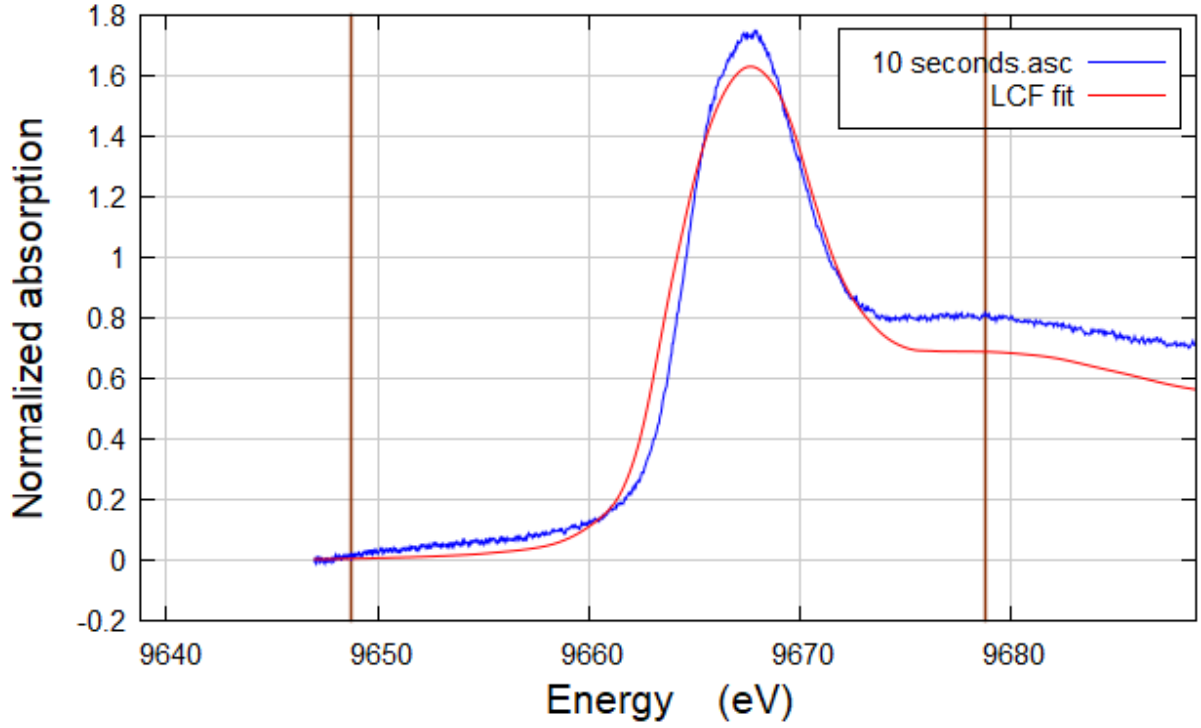

Figure S18: LCF of spectrum at 10 seconds

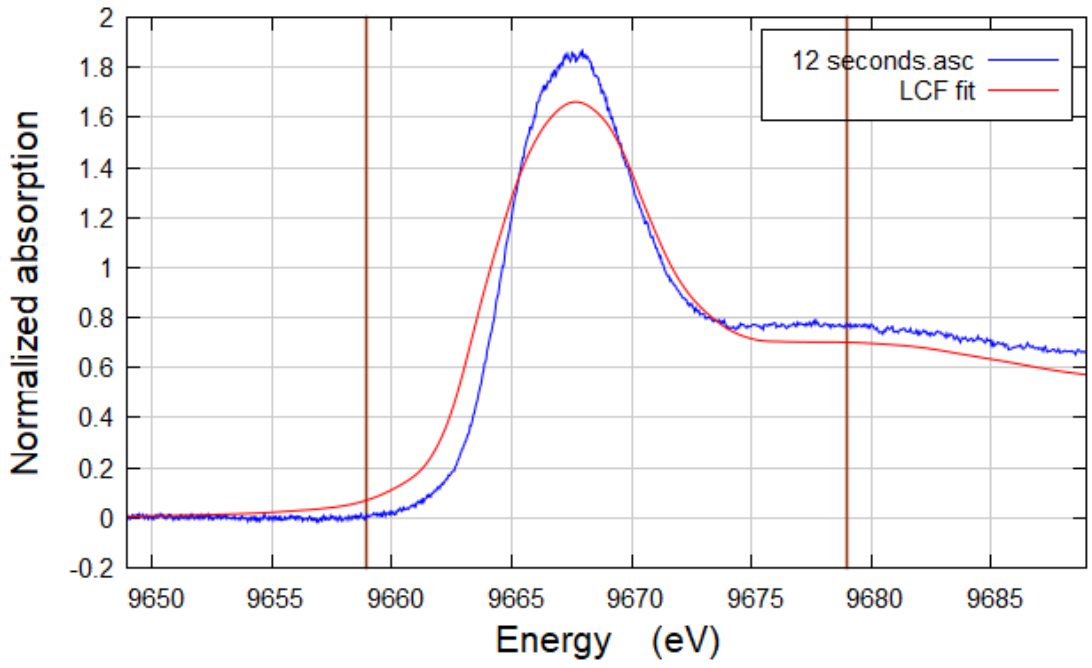

Figure S19: LCF of spectrum at 12 seconds

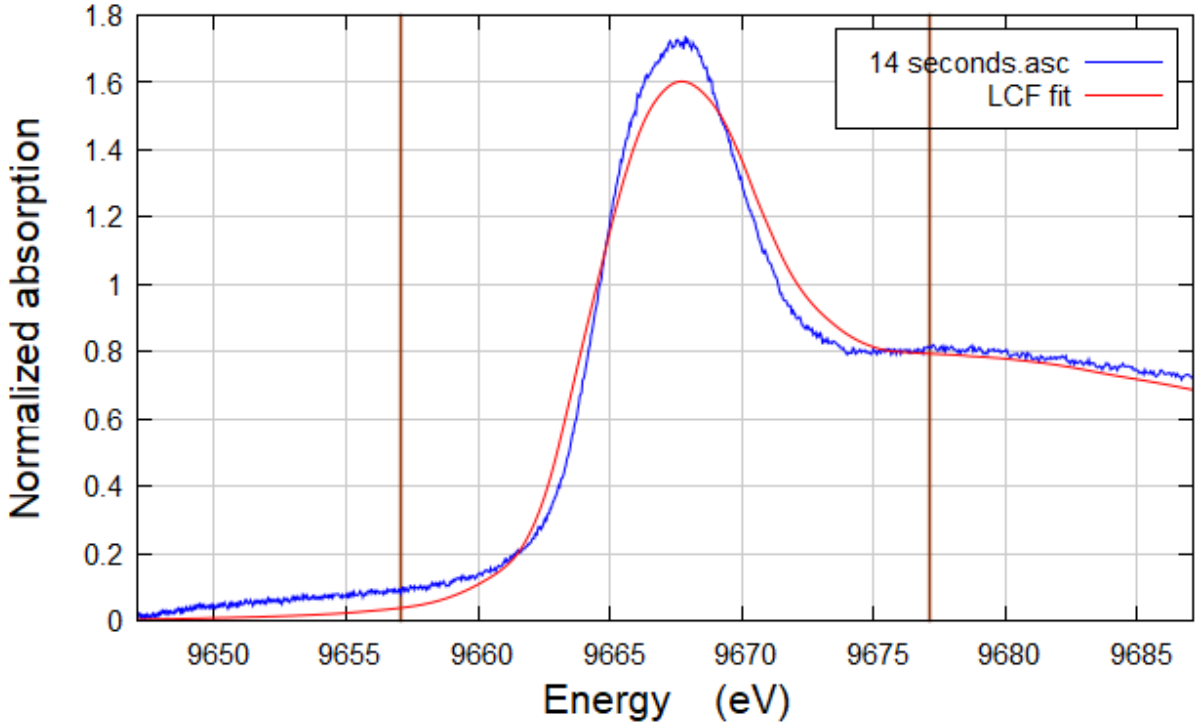

Figure S20: LCF of spectrum at 14 seconds

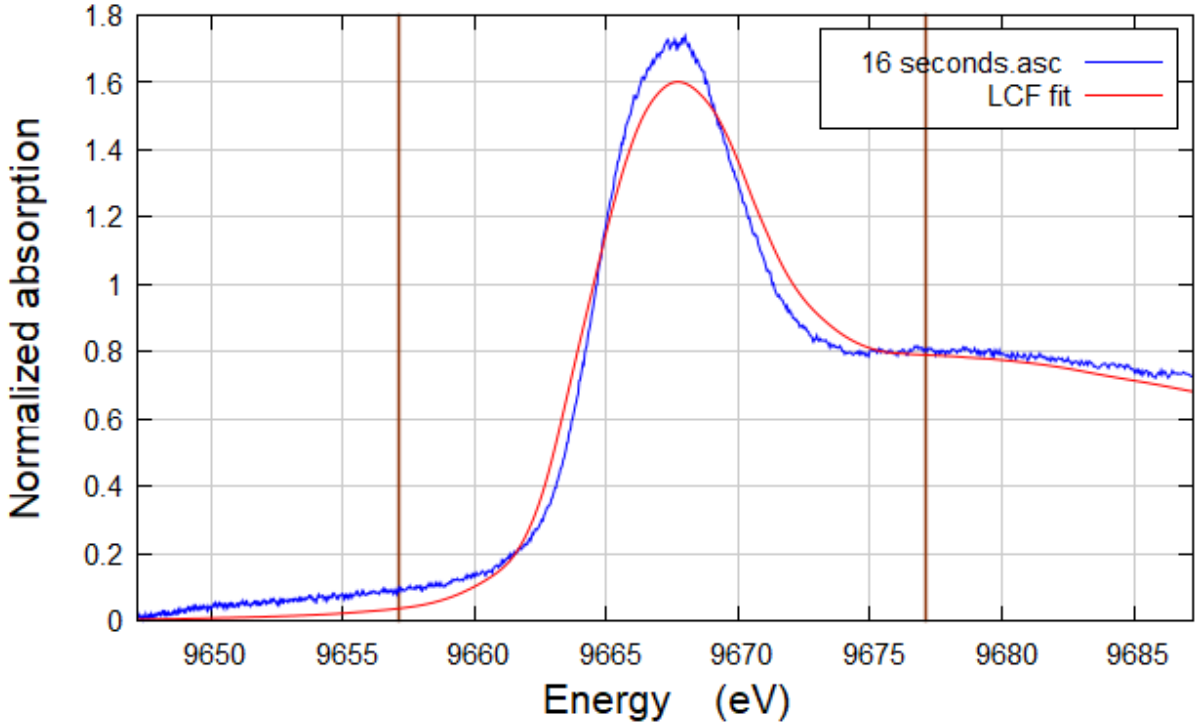

Figure S21: LCF of spectrum at 16 seconds

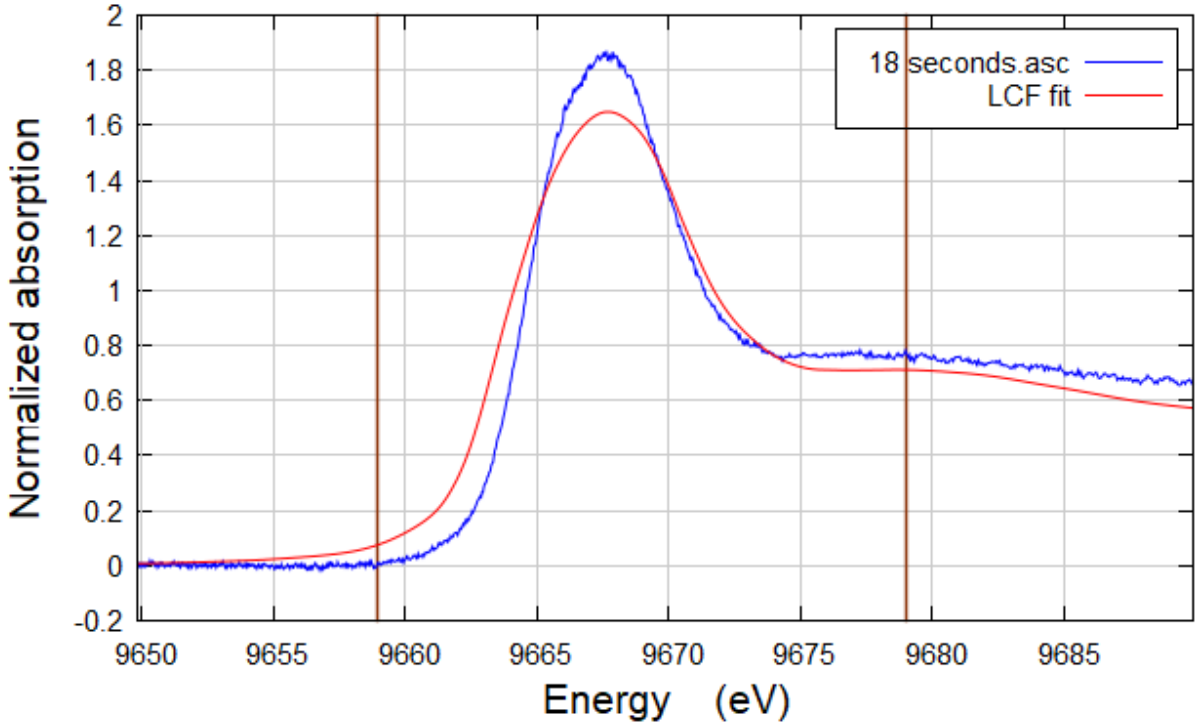

Figure S22: LCF of spectrum at 18 seconds

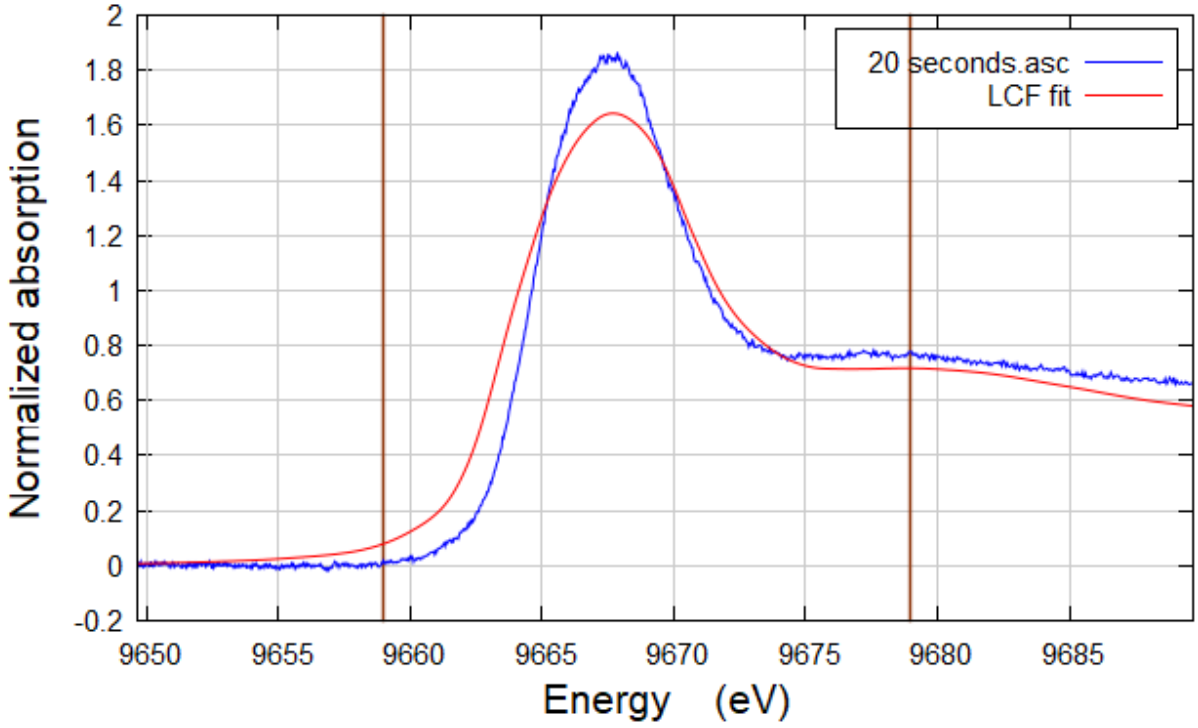

Figure S23: LCF of spectrum at 20 seconds

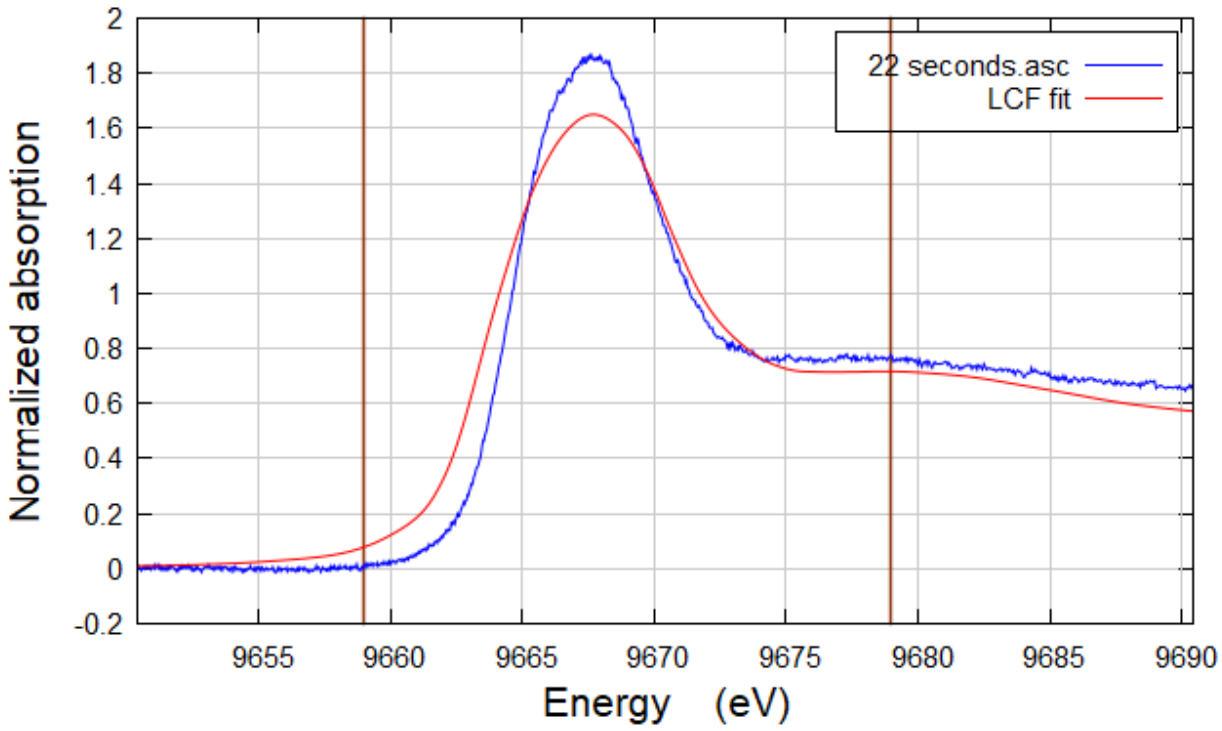

Figure S24: LCF of spectrum at 22 seconds

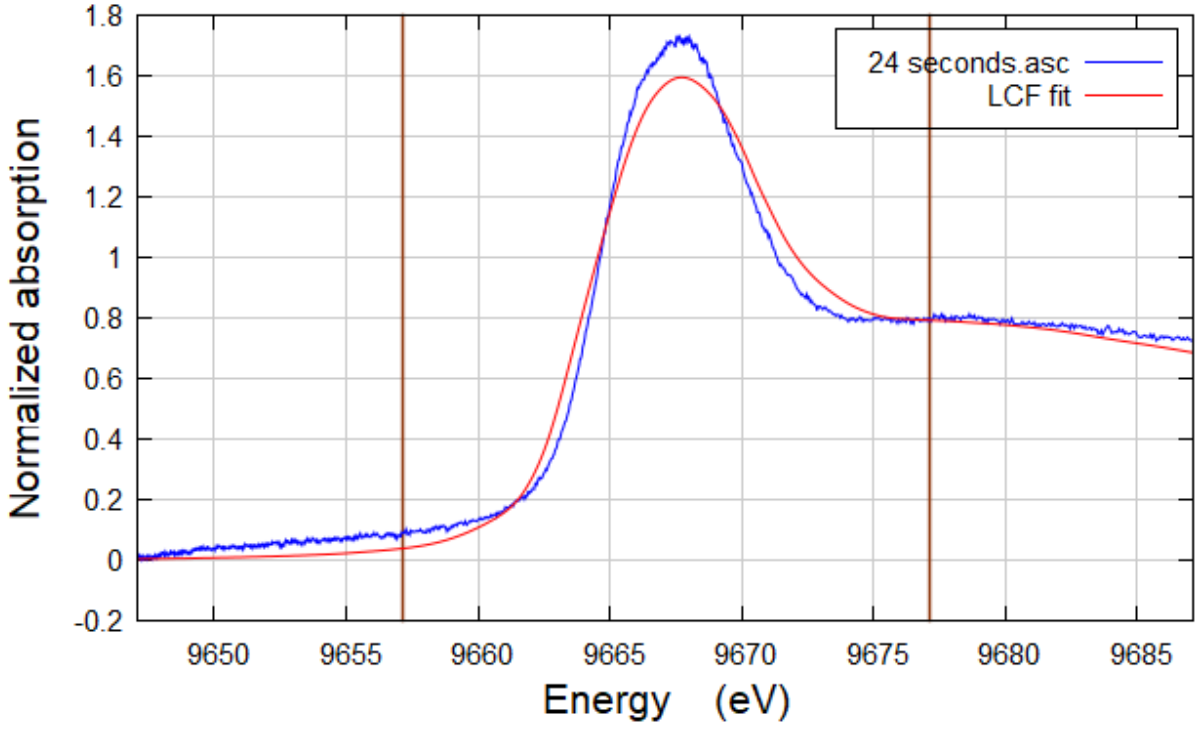

Figure S25: LCF of spectrum at 24 seconds

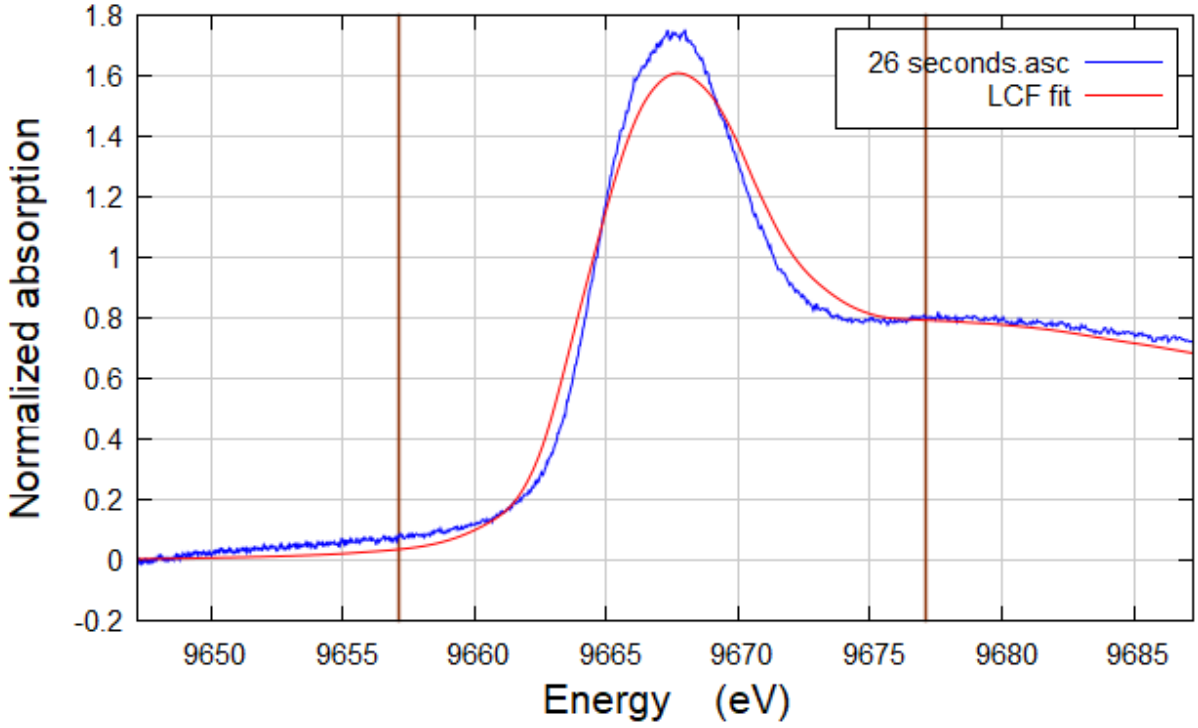

Figure S26: LCF of spectrum at 26 seconds

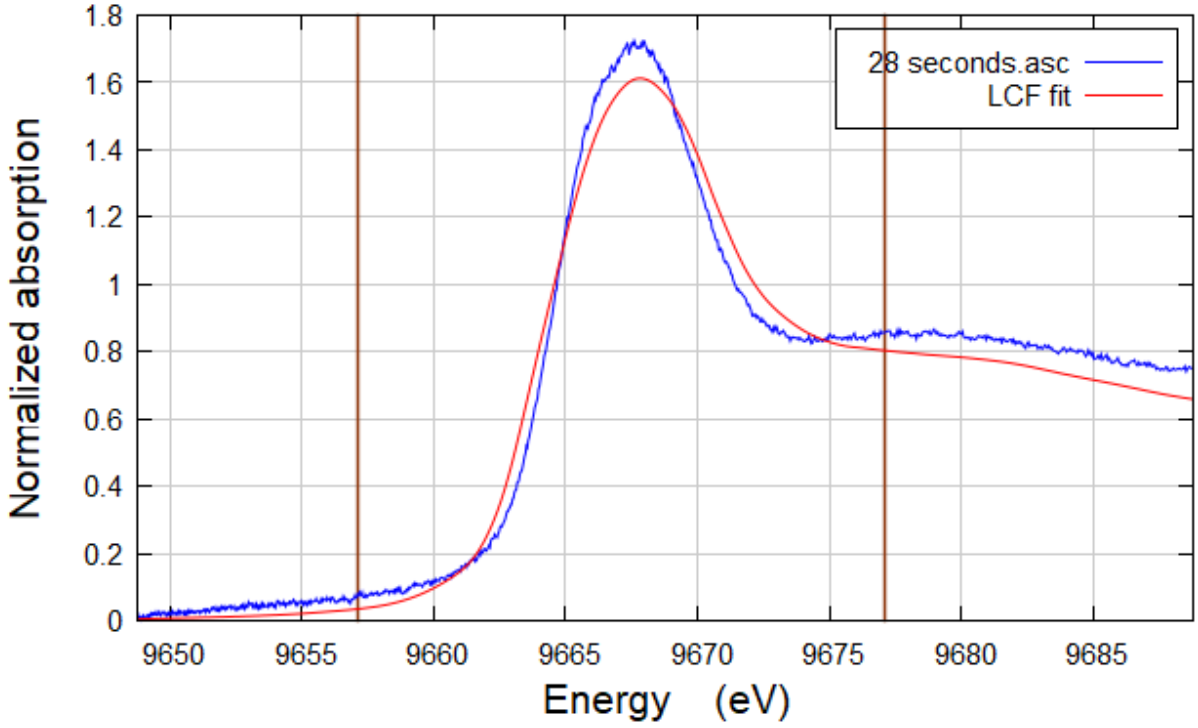

Figure S27: LCF of spectrum at 28 seconds

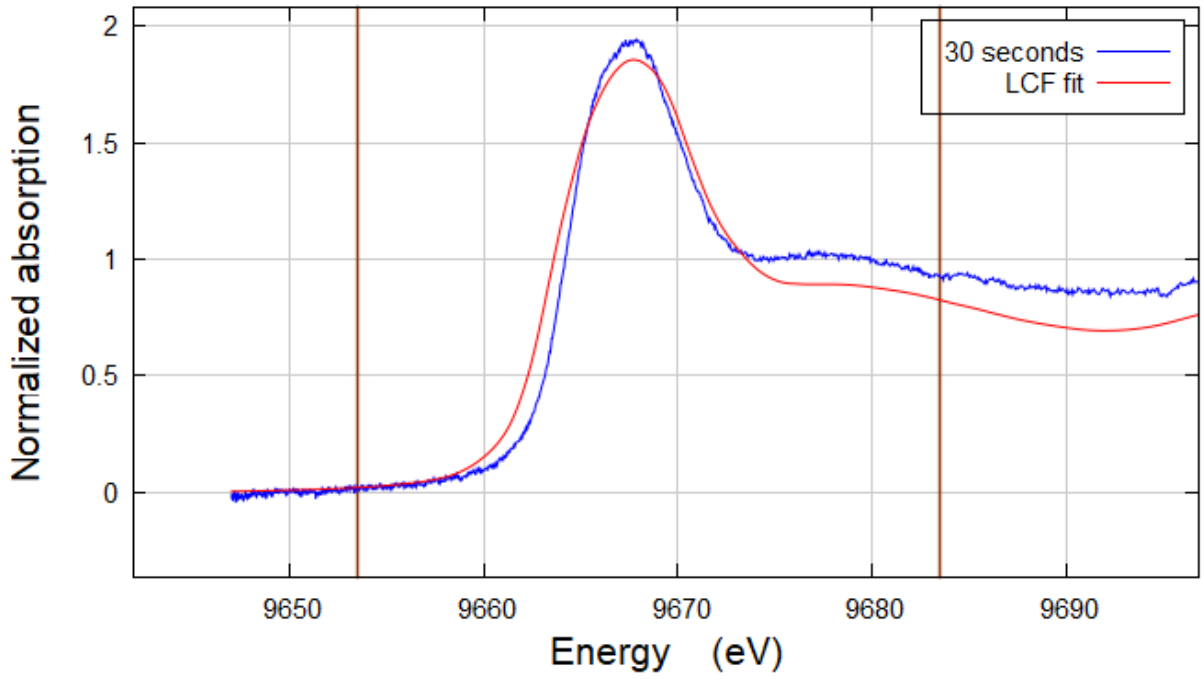

Figure S28: LCF of spectrum at 30 seconds

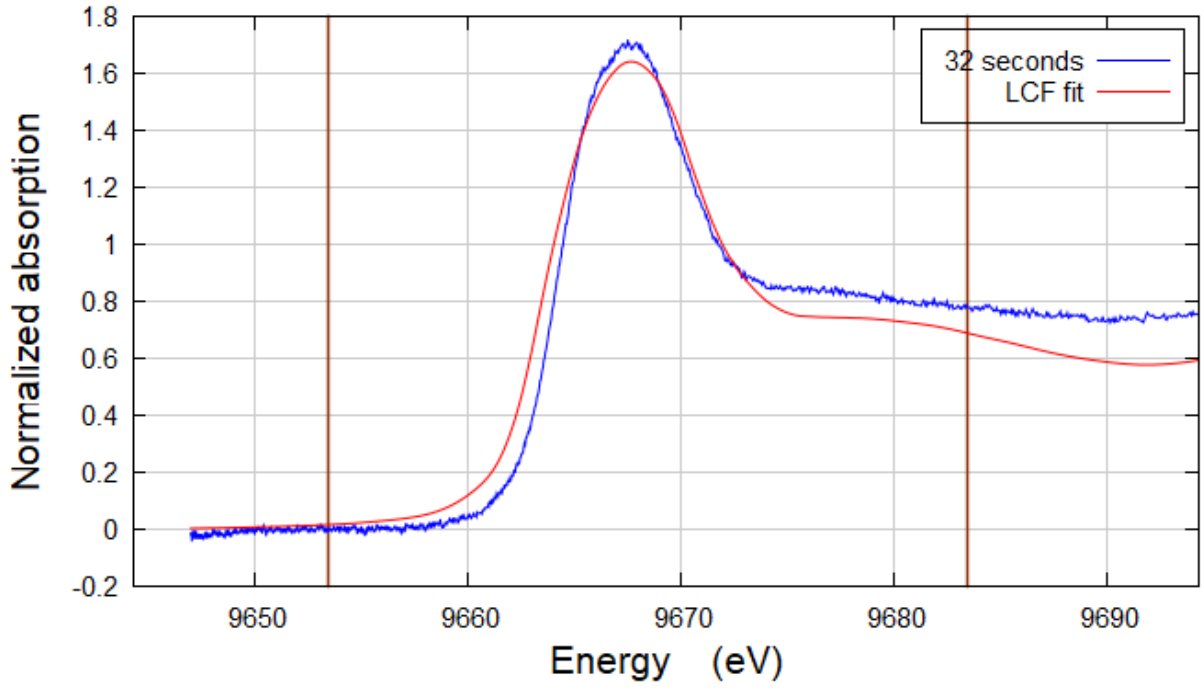

Figure S29: LCF of spectrum at 32 seconds

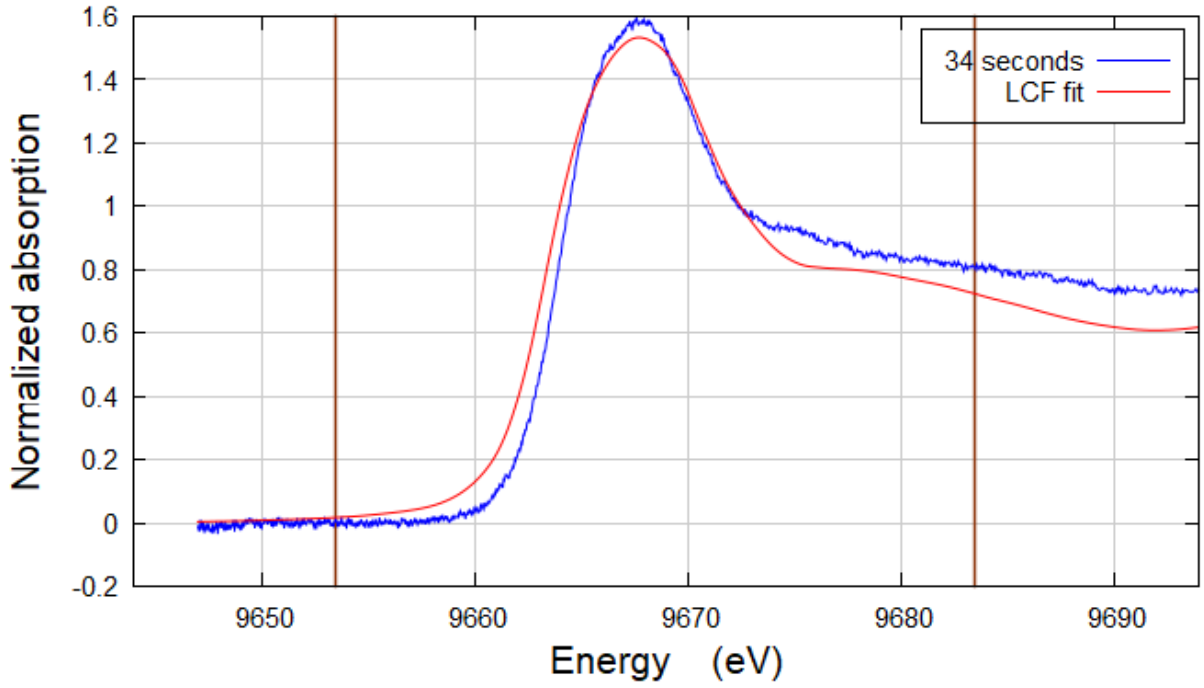

Figure S30: LCF of spectrum at 34 seconds

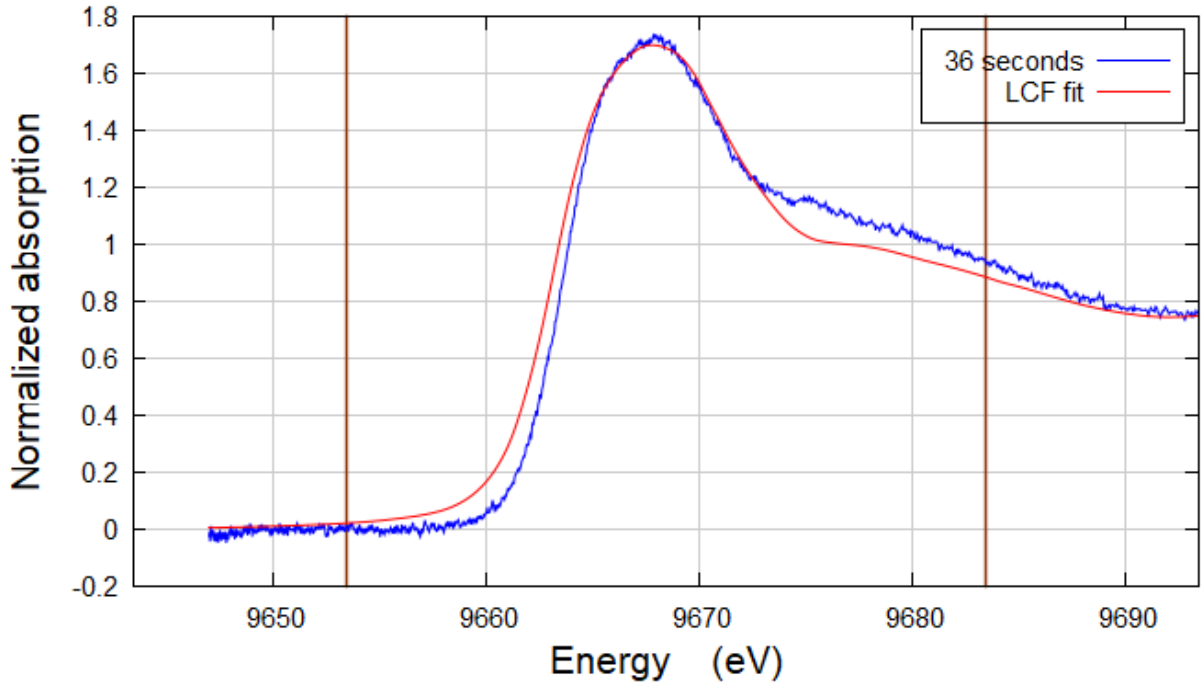

Figure S31: LCF of spectrum at 36 seconds

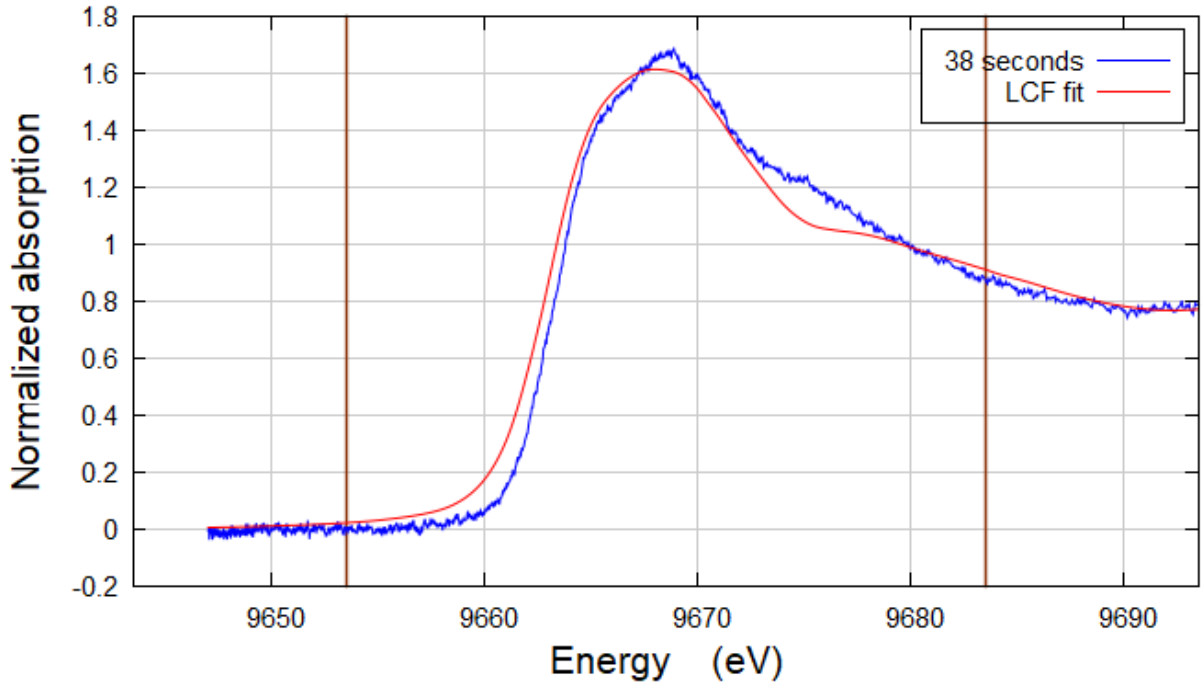

Figure S32: LCF of spectrum at 38 seconds

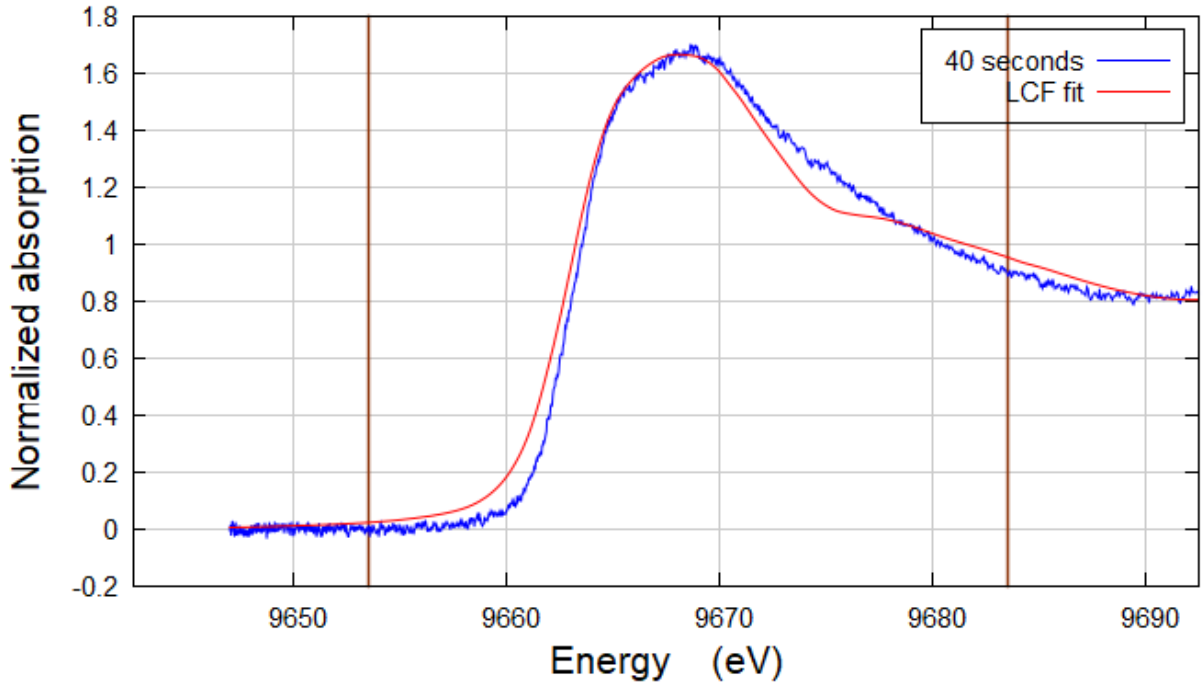

Figure S33: LCF of spectrum at 40 seconds

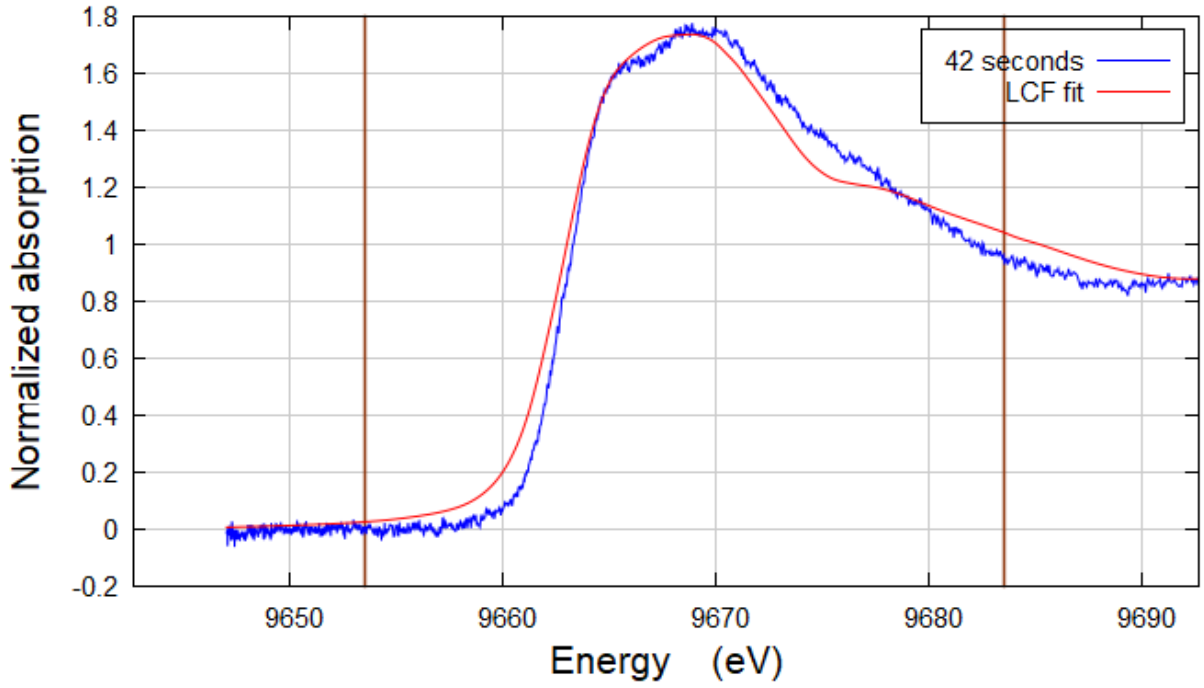

Figure S34: LCF of spectrum at 42 seconds

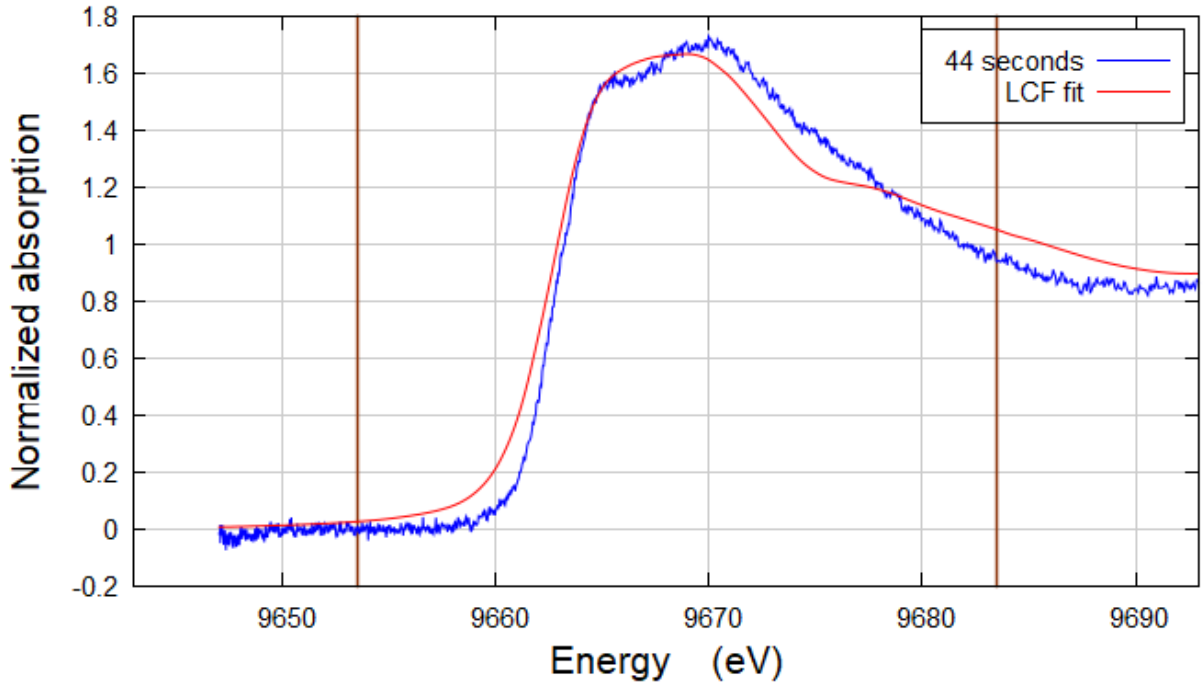

Figure S35: LCF of spectrum at 44 seconds

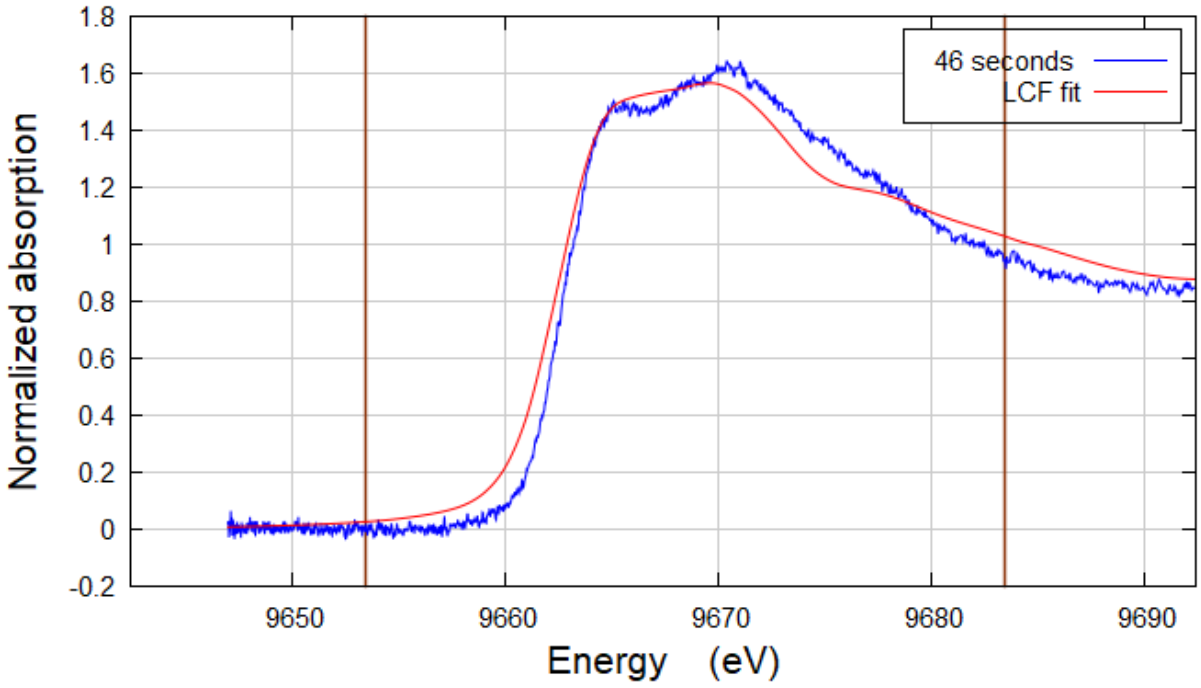

Figure S64: LCF of spectrum at 46 seconds

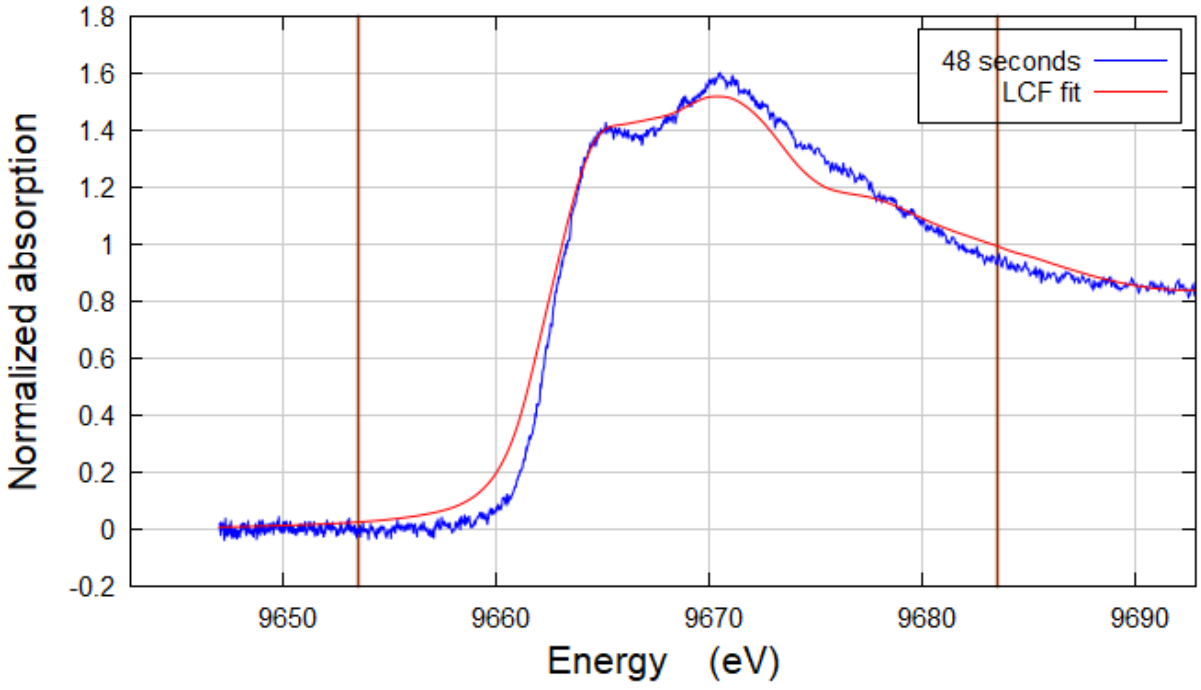

Figure S37: LCF of spectrum at 48 seconds

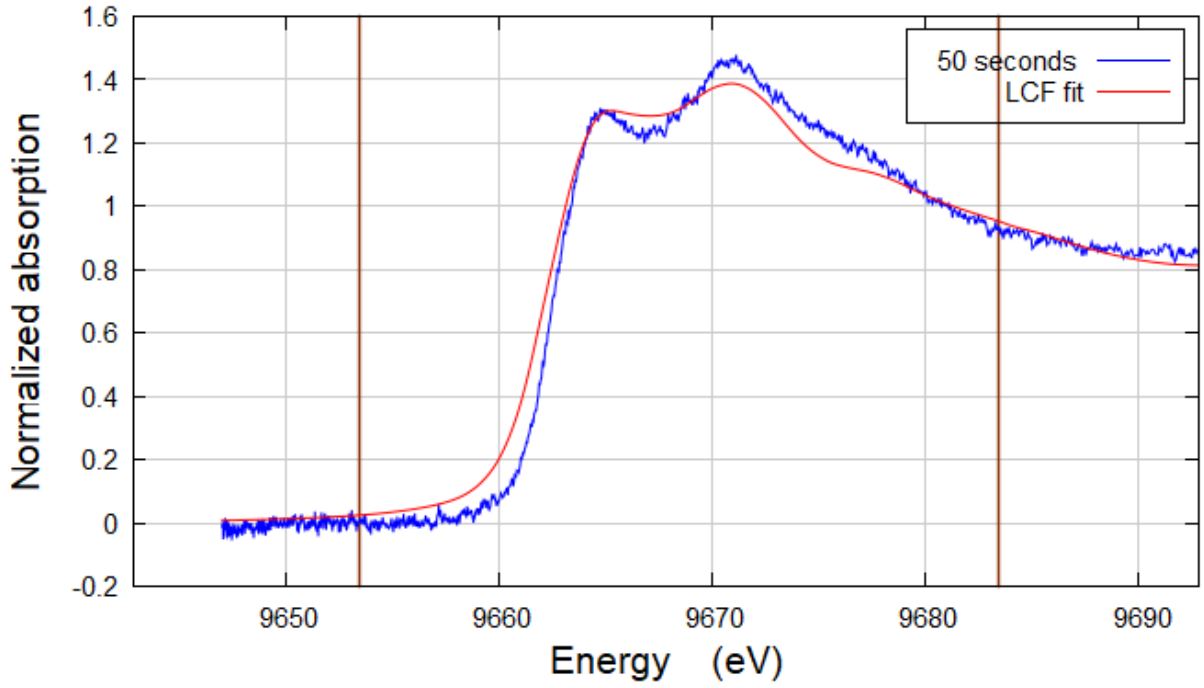

Figure S38: LCF of spectrum at 50 seconds

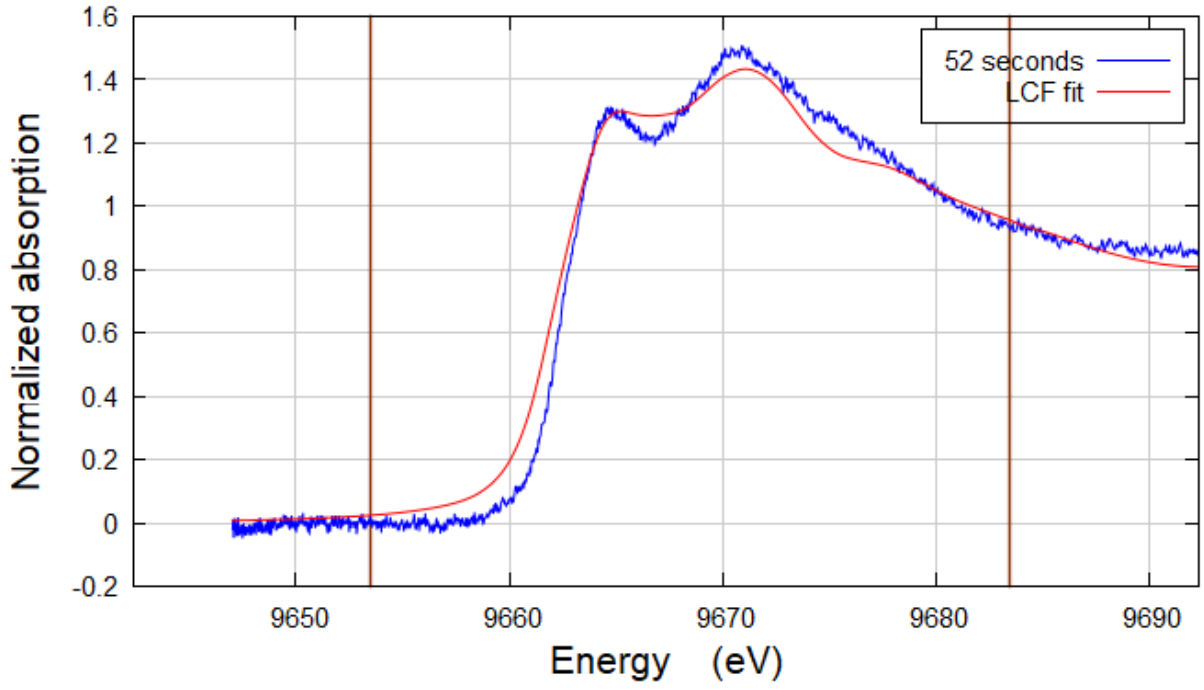

Figure S39: LCF of spectrum at 52 seconds

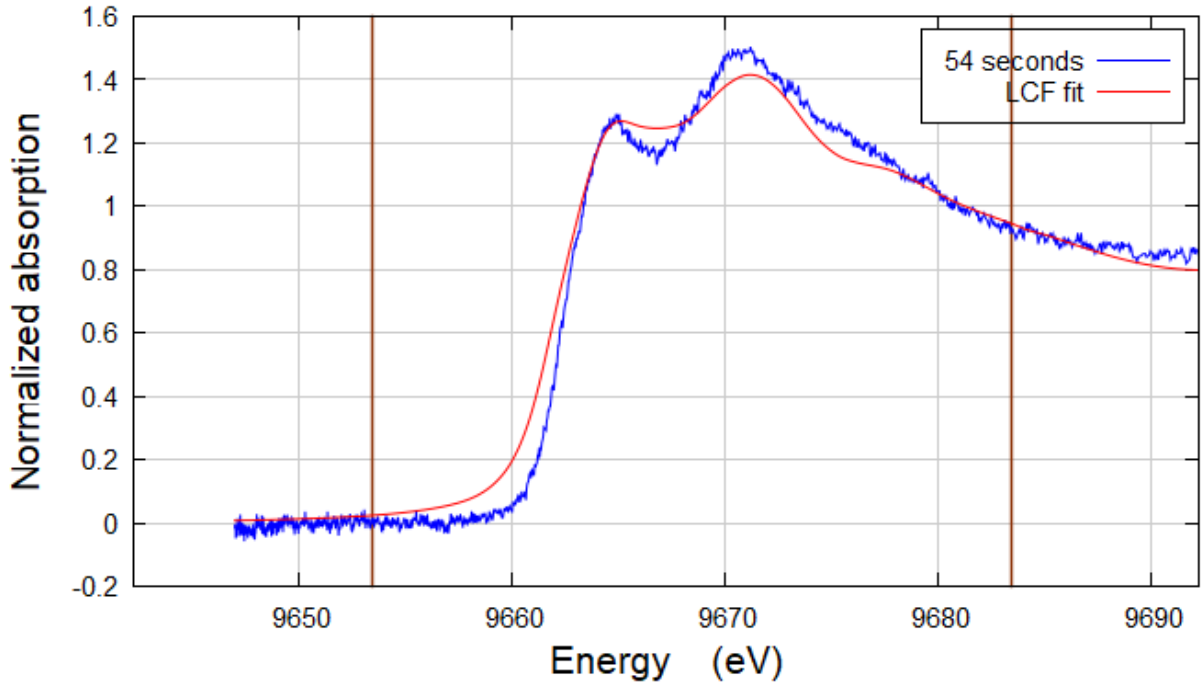

Figure S40: LCF of spectrum at 54seconds

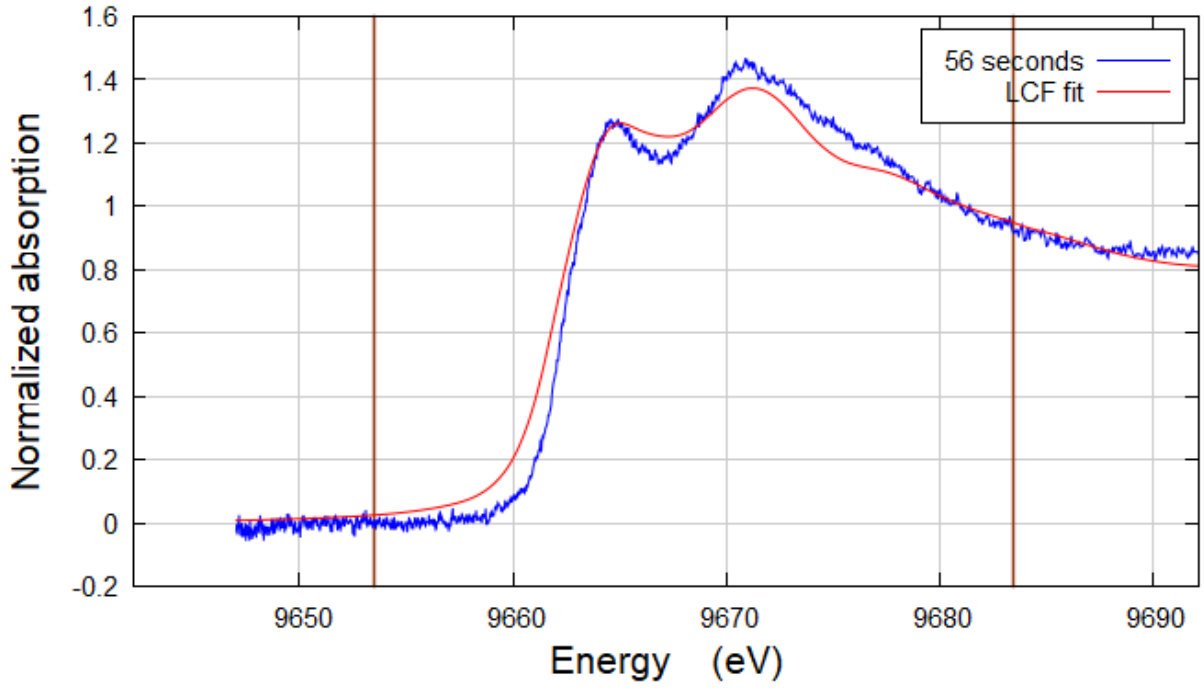

Figure S41: LCF of spectrum at 56 seconds

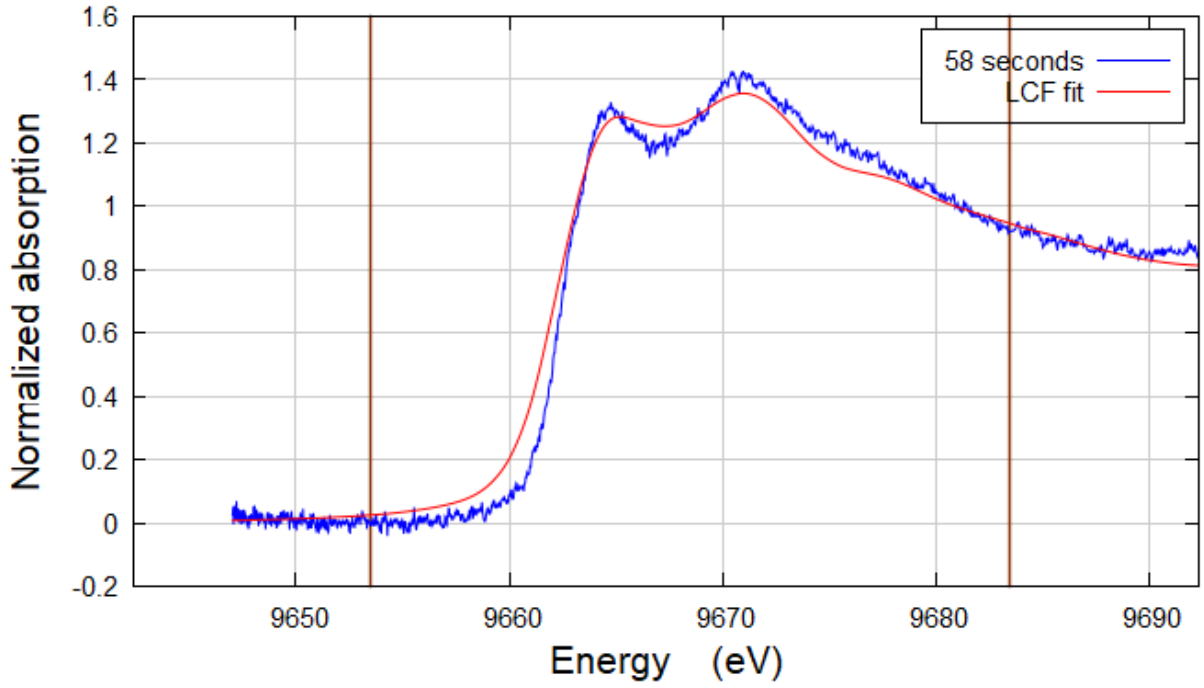

Figure S42: LCF of spectrum at 58 seconds

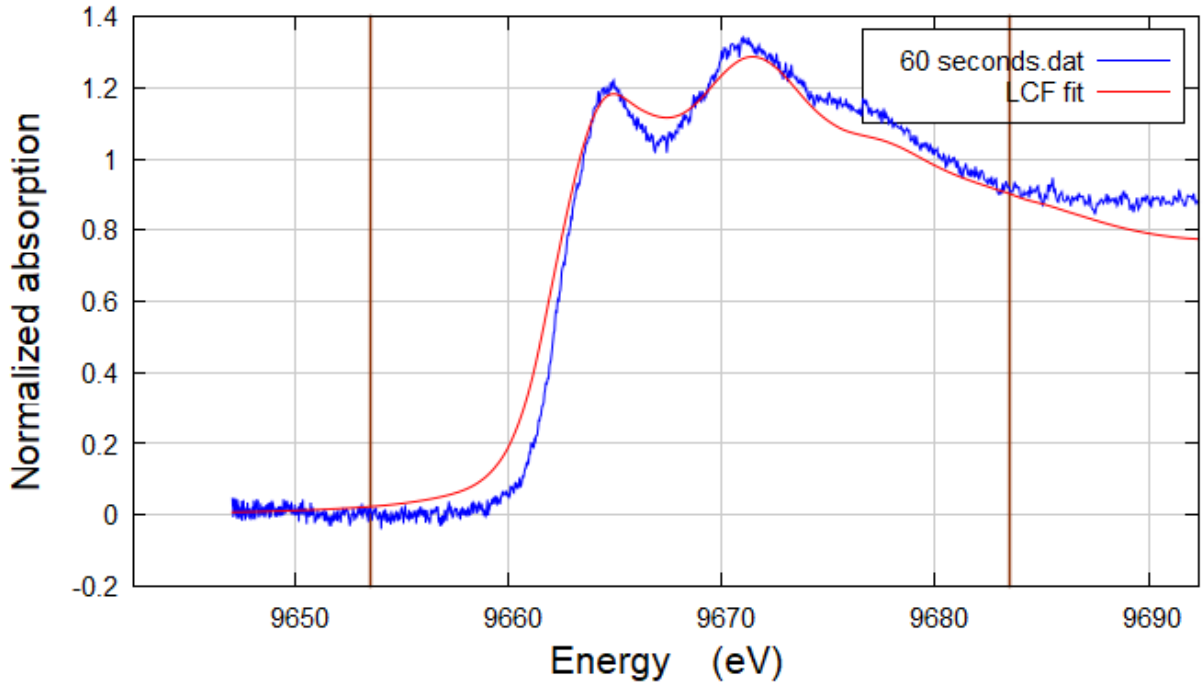

Figure S43: LCF of spectrum at 60 seconds

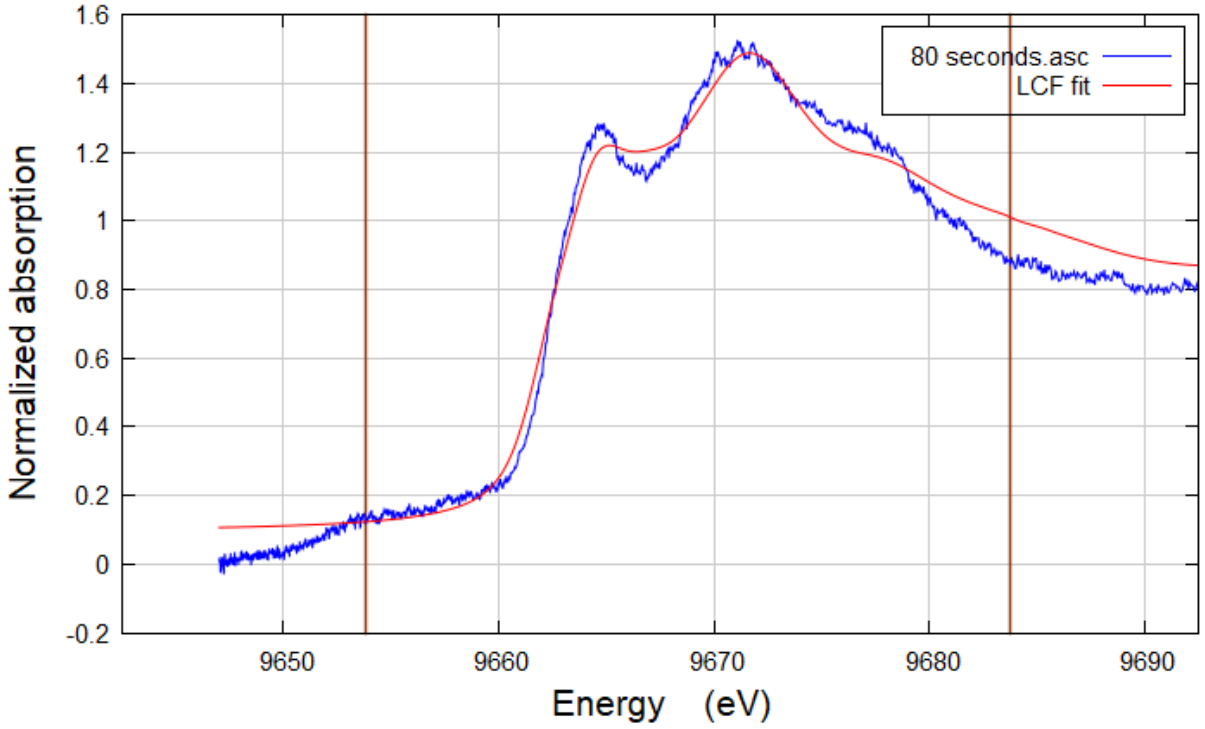

Figure S44: LCF of spectrum at 80 seconds

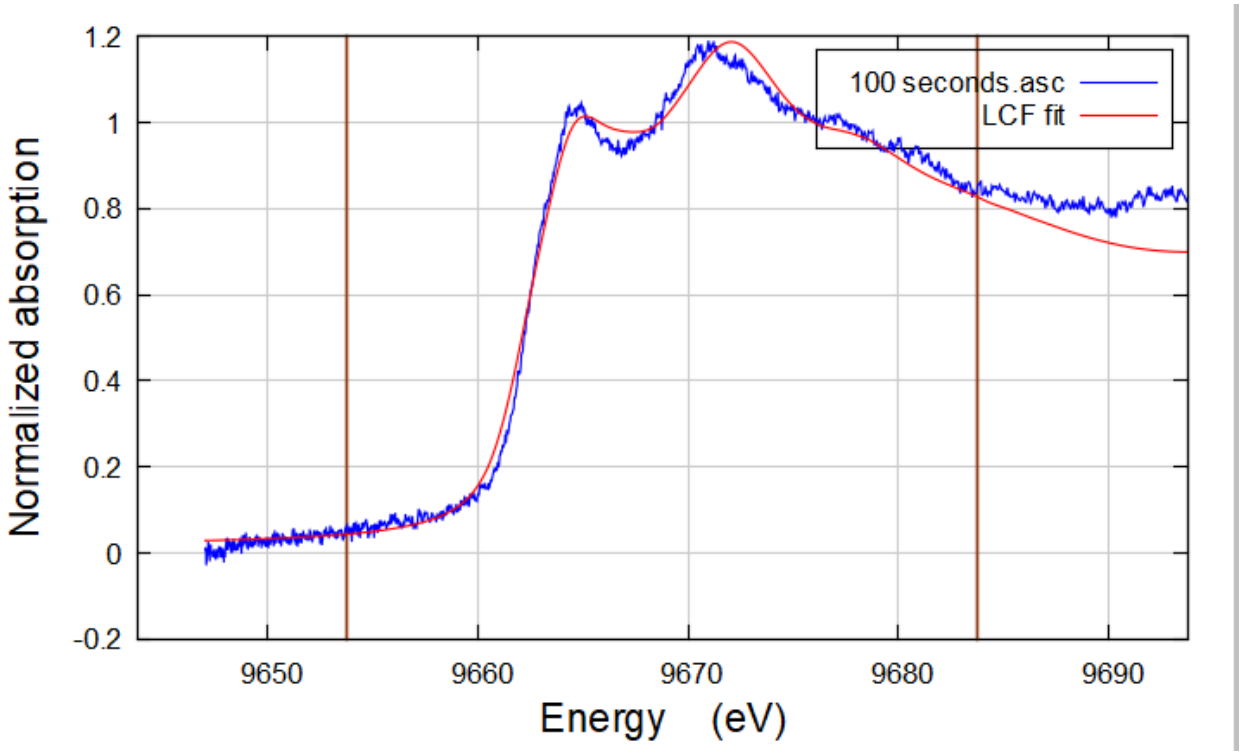

Figure S45: LCF of spectrum at 100 seconds

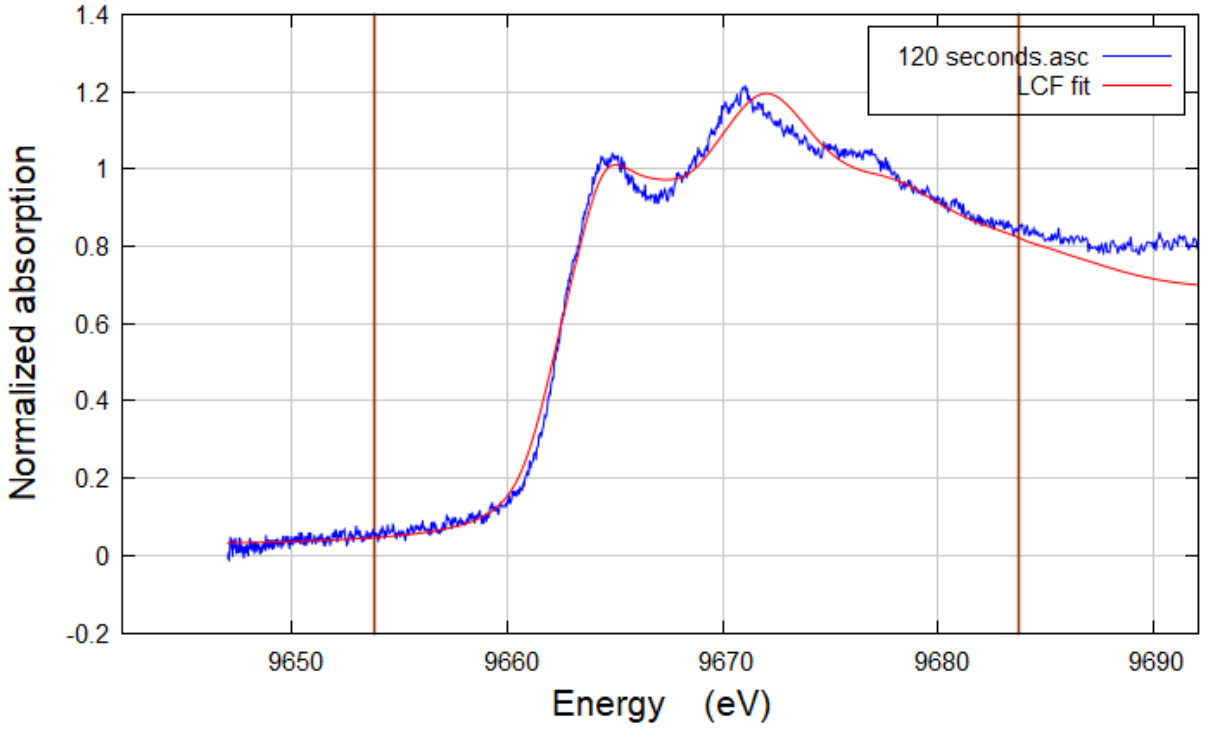

Figure S46: LCF of spectrum at 120 seconds

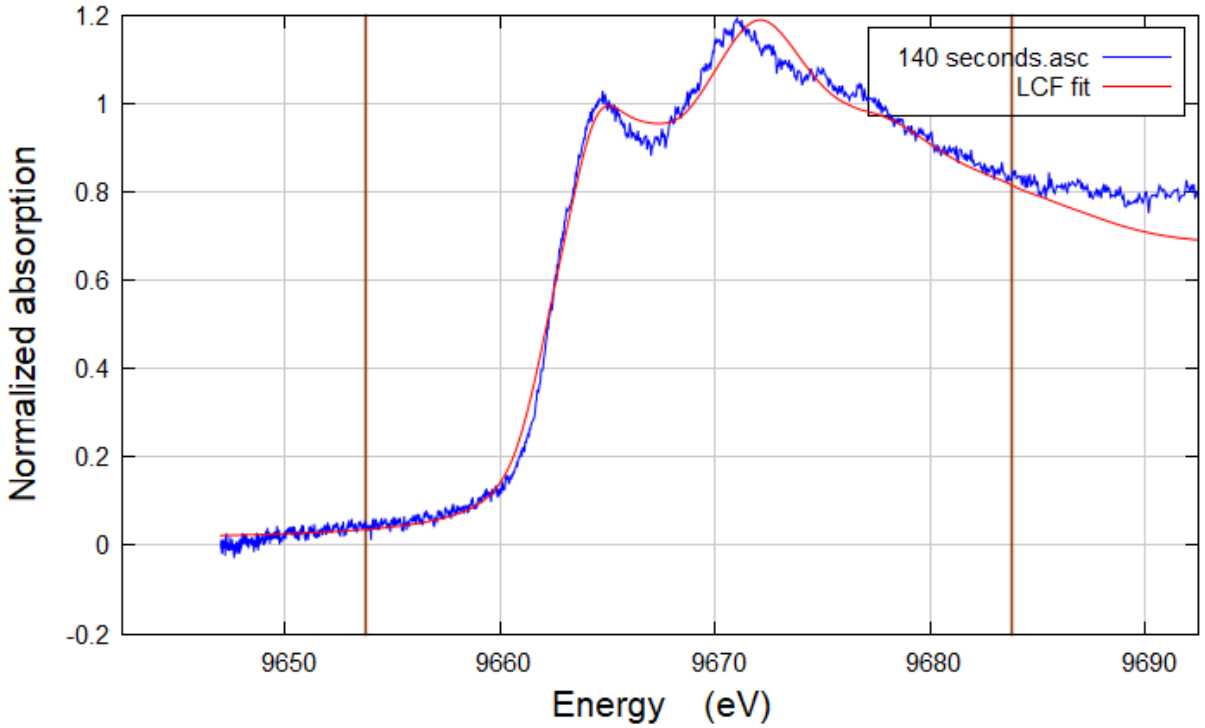

Figure S47: LCF of spectrum at 140 seconds

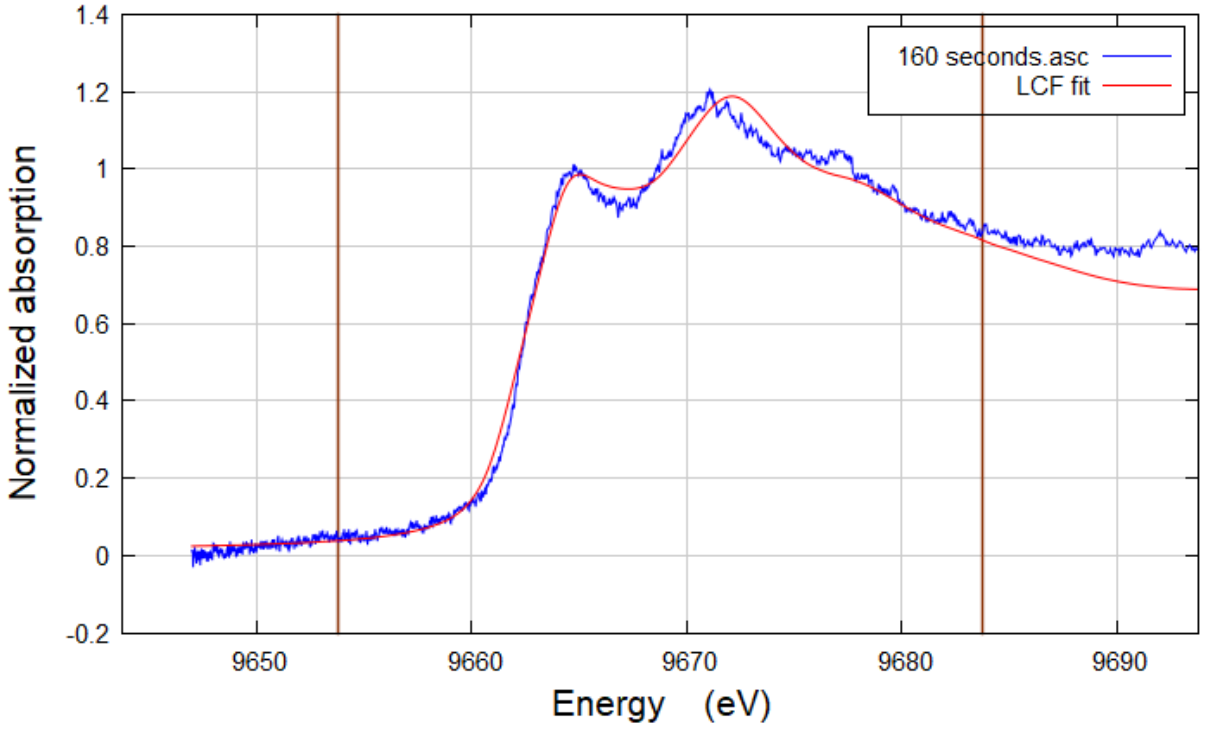

Figure S48: LCF of spectrum at 160 seconds

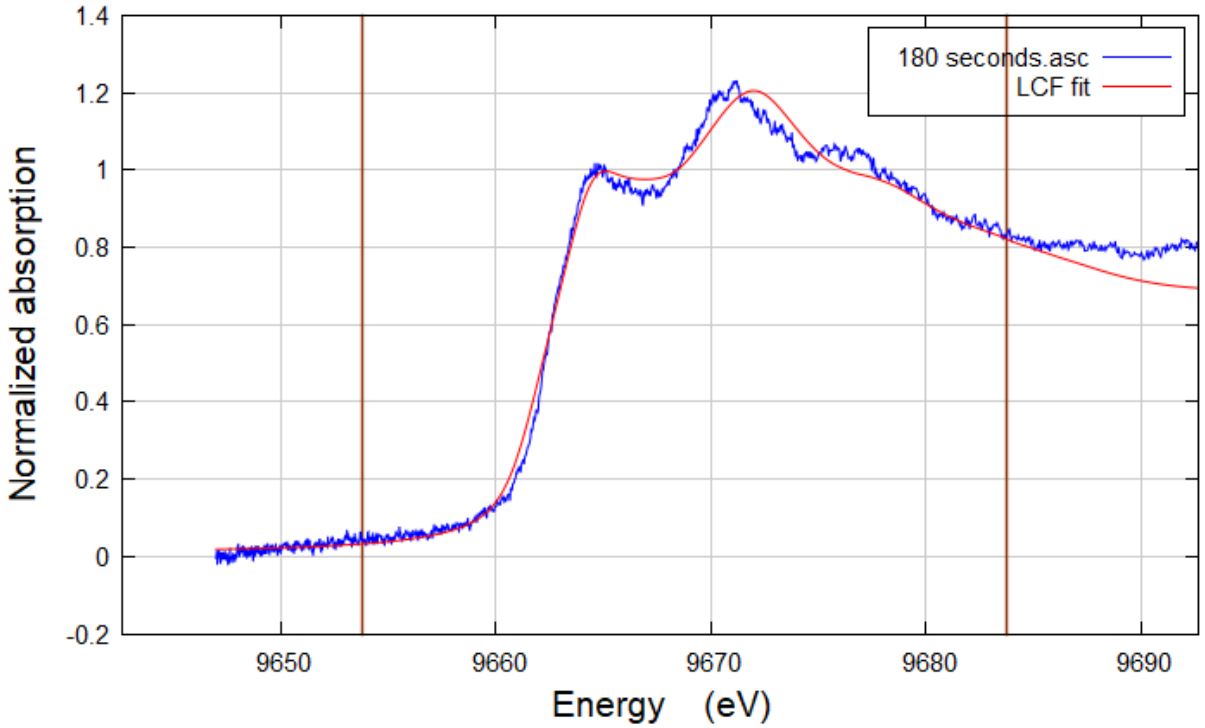

Figure S49: LCF of spectrum at 180 seconds

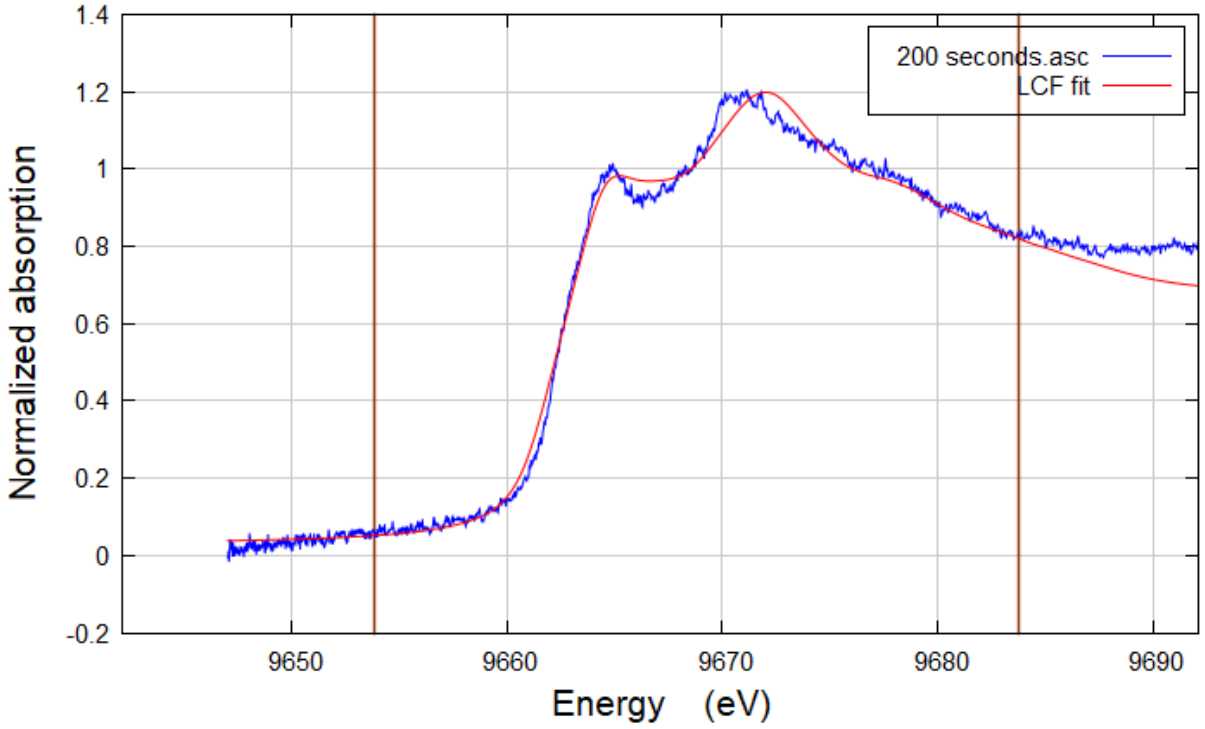

Figure S50: LCF of spectrum at 200 seconds

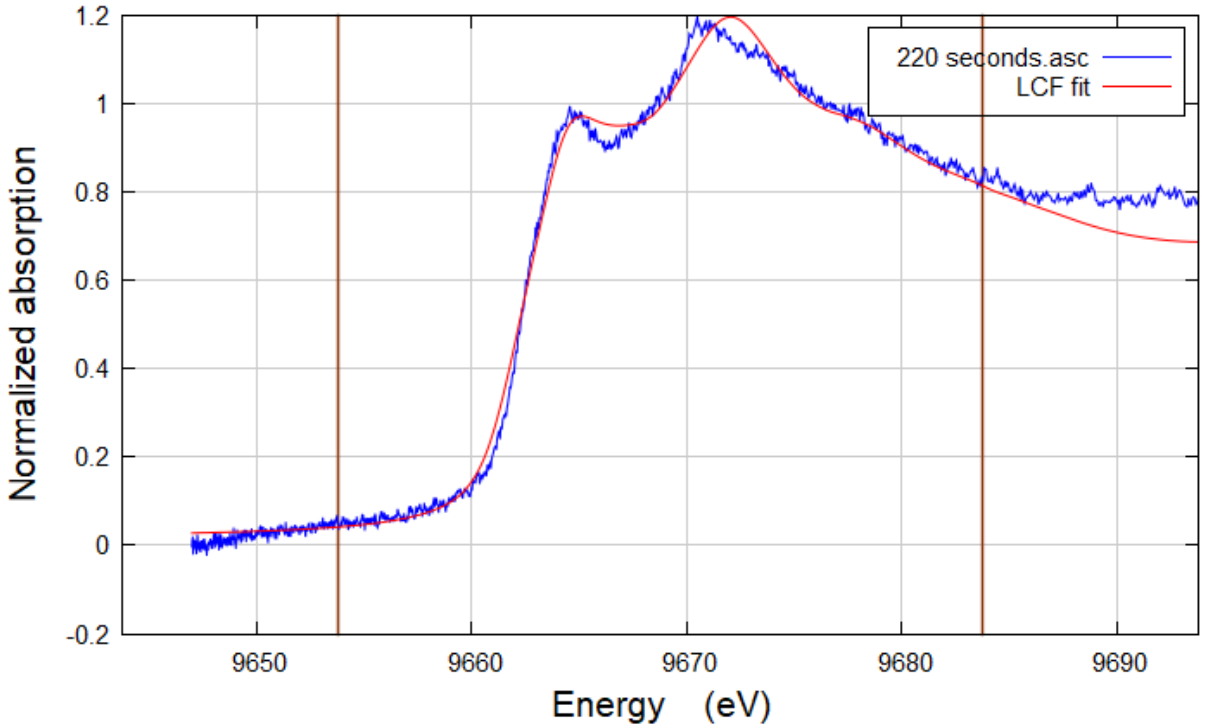

Figure S51: LCF of spectrum at 220 seconds

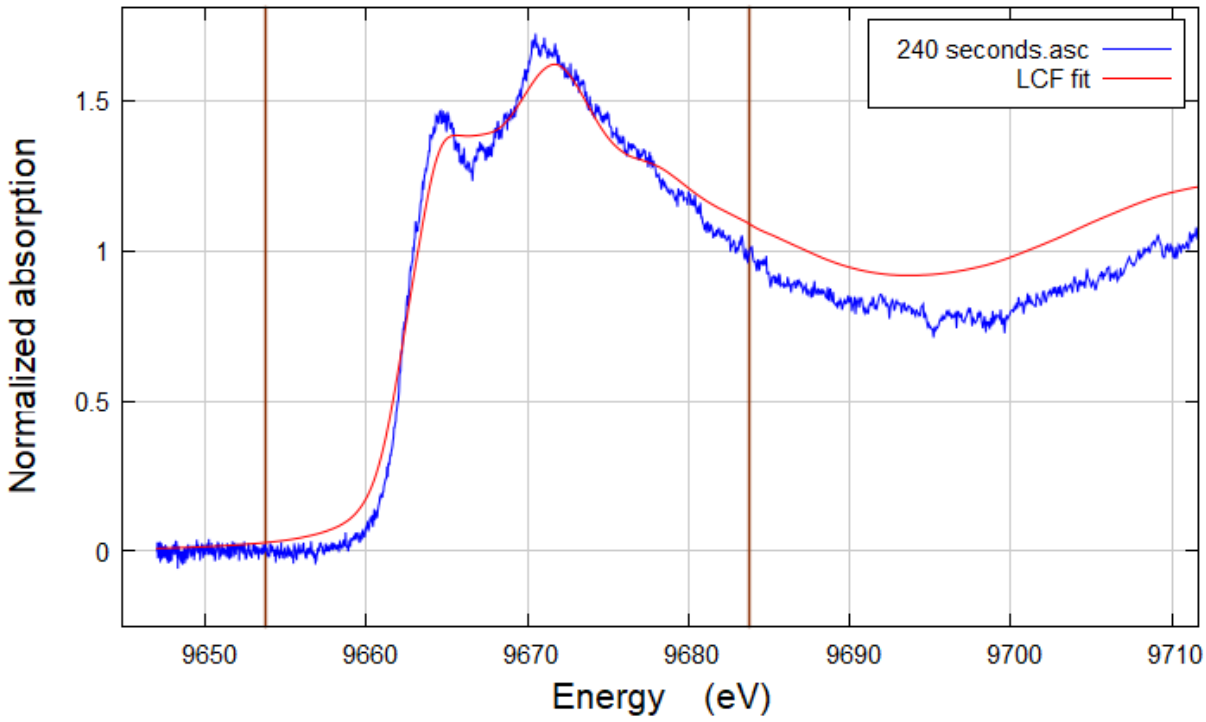

Figure S52: LCF of spectrum at 240 seconds

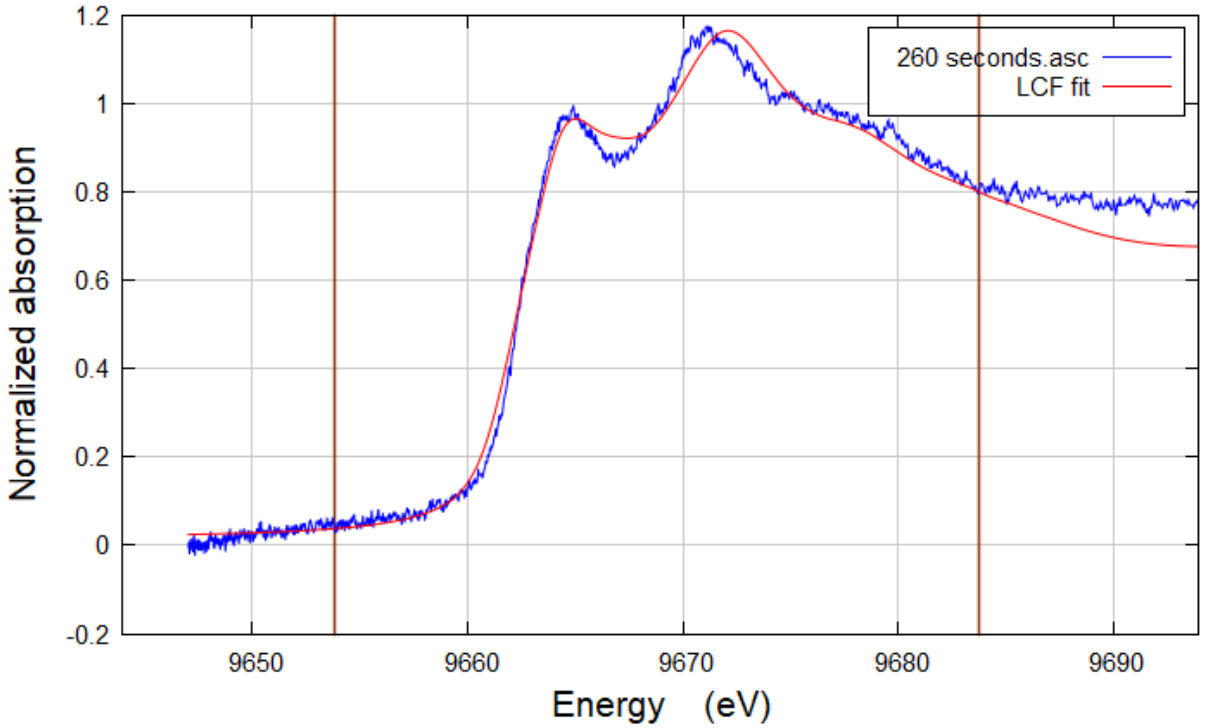

Figure S53: LCF of spectrum at 26 seconds

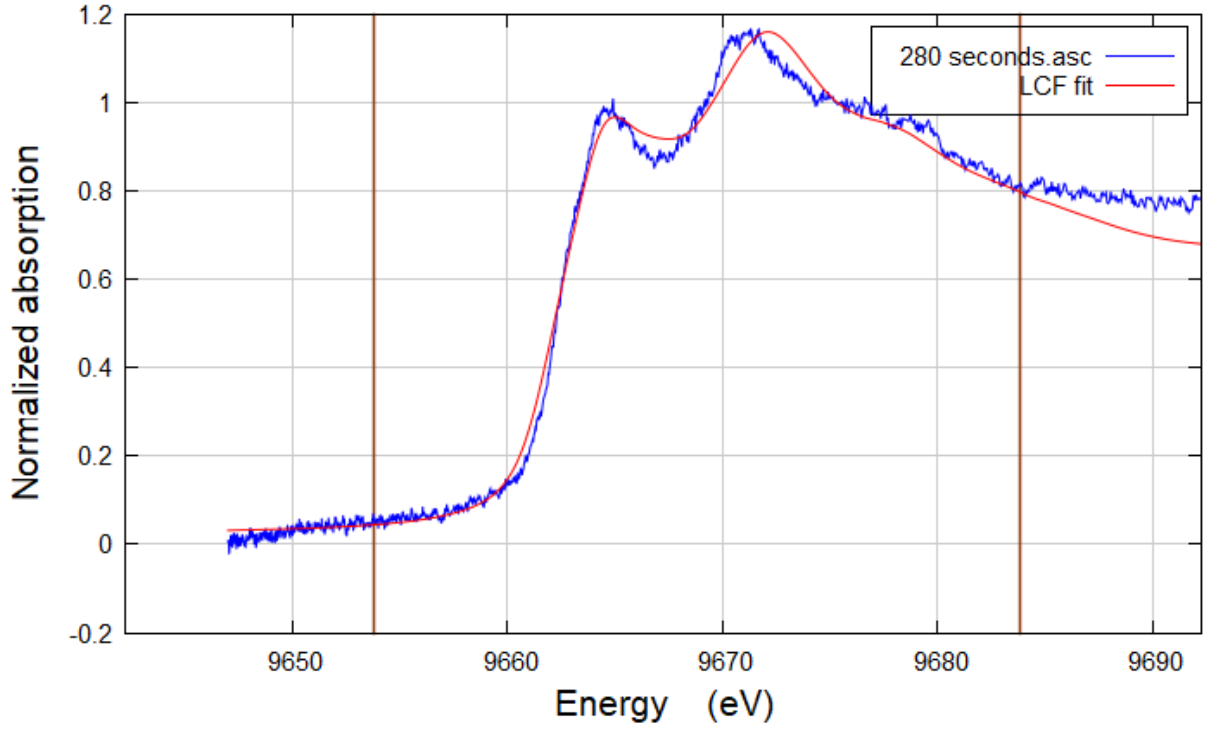

Figure S54: LCF of spectrum at 280 seconds

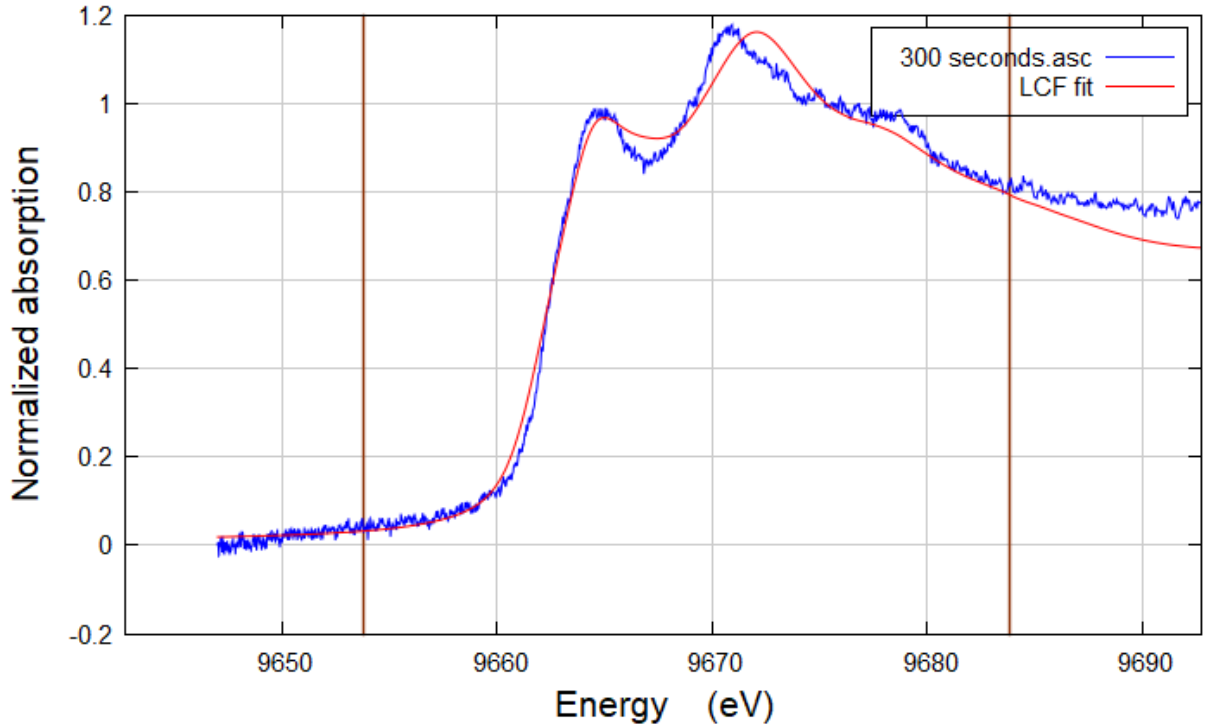

Figure S55: LCF of spectrum at 300 seconds

						ZIF-8					Dichlorobis(1-MeIM)zinc(II)			
Data	rfactor	chinu	chisqr	nv ary	scale by	weight	error	e0	error	weight	error	e0	error	
2 seconds.dat	0.0318555	0.010498	8.06249	5	0.79	0.045370025	0.071449622	0	0.131271984	1.04662E-06	0.045850637	0	0.1477407	
4 seconds.asc	0.0398551	0.0132073	10.1432	5	0.73	2.68106E-09	0.080140362	0	0.131271984	5.81799E-08	0.051427612	0	0.1477407	
6 seconds.asc	0.0159443	0.0046358	5.06692	5	0.709	1.99E-06	0.082571263	0	3.368882861	6.38E-08	0.042648479	0	0.290724859	
8 seconds.asc	0.0155452	0.0045996	5.02733	5	0.709	9.54E-09	0.082247894	0	3.368882861	4.70E-08	0.042481454	0	0.290724859	
10 seconds.asc	0.0158369	0.004642	5.07366	5	0.709	9.54E-09	0.082624904	0	3.368882861	4.70E-08	0.042676945	0	0.290724859	
12 seconds.asc	0.0567664	0.0192728	9.73275	5	0.722	2.68E-08	0.158958946	0	49068.04722	3.78E-08	0.085220454	0	2.040670324	
14 seconds.asc	0.0179228	0.0055388	2.90231	10	0.784	6.38E-07	0.11743195	3.357607864	162135.2043	0.206309376	0.158647414	2.811392505	0.367178058	
16 seconds.asc	0.0179799	0.0055492	2.90777	10	0.782	3.90E-08	0.114633263	3.335028431	2667710.501	0.208272606	0.157234926	2.813927103	0.371548204	
18 seconds.asc	0.0606528	0.0205875	10.39669	5	0.727	2.82E-07	0.164290079	0	49068.04722	2.54E-07	0.088078395	0	2.040670324	
20 seconds.asc	0.0630022	0.0213053	10.75919	5	0.73	1.16E-08	0.167130852	0	49068.04722	2.47E-08	0.089601091	0	2.040670324	
22 seconds.asc	0.0619328	0.0212279	10.72009	5	0.73	9.68E-06	0.16682571	0	49068.04722	8.29E-06	0.089437773	0	2.040670324	
24 seconds.asc	0.0182416	0.0056317	2.95099	10	0.782	2.79E-08	0.131569259	3.18463407	3465414.874	0.209435138	0.159200637	2.784411847	0.379263517	
26 seconds.asc	0.0188279	0.0060525	3.17149	10	0.785	4.64E-08	0.128212239	3.555614309	1784927.978	0.210598263	0.174350855	2.781179751	0.483394854	
28 seconds.asc	0.0152077	0.0047935	2.51179	10	0.784	0.054057422	0.093723984	3.406082379	1.807812866	0.141596594	0.126256315	2.86161543	0.771260537	
30 seconds	0.0282043	0.0113234	9.07007	5	0.887	0.116647312	0.074893062	0	0	1.03E-08	0.049604923	0	0	
32 seconds	0.0244495	0.0078318	6.27325	5	0.75	0.066505622	0.062284842	0	0	4.18E-08	0.041254633	0	0	
34 seconds	0.023157	0.0070049	5.61094	5	0.78	0.186901196	0.05890548	0	0	6.23E-06	0.039016172	0	0	
36 seconds	0.0208546	0.0082569	6.61381	5	0.942	0.301221825	0.063953416	0	0	2.35E-08	0.042359524	0	0	
38 seconds	0.0186855	0.007178	5.74958	5	0.961	0.350252252	0.059628782	0	0	1.06E-08	0.039495251	0	0	
40 seconds	0.0148145	0.006117	4.89972	5	1.007	0.39119484	0.055045669	0	0	1.43E-08	0.036459667	0	0	
42 seconds	0.01521	0.0071638	5.73818	5	1.094	0.475819113	0.059569646	0	0	1.89E-08	0.039456055	0	0	
44 seconds	0.0197314	0.0089987	7.20797	5	1.094	0.389303499	0.066764308	0	0	0.127190064	0.04422149	0	0	
46 seconds	0.0180073	0.0074402	5.95957	5	1.065	0.417239581	0.060707907	0	0	0.132944723	0.040210014	0	0	
48 seconds	0.0155456	0.0059986	4.80491	5	1.034	0.581504282	0.054511514	0	0	3.03E-07	0.03610533	0	0	
50 seconds	0.0173071	0.0056688	4.54073	5	0.979	0.46030783	0.052990845	0	0	0.134180889	0.035098601	0	0	
52 seconds	0.0164976	0.0056443	4.52108	5	0.99	0.609222727	0.052876032	0	0	0.010494556	0.035022555	0	0	
54 seconds	0.0186932	0.0062081	4.97272	5	0.977	0.621120507	0.055454244	0	0	9.00E-05	0.036730239	0	0	
56 seconds	0.0194597	0.0061997	4.966	5	0.972	0.496177288	0.055416753	0	0	0.128865763	0.036705406	0	0	
58 seconds	0.0161209	0.0050471	4.04275	5	0.97	0.423094567	0.050000729	0	0	0.188559872	0.033118091	0	0	
60 seconds.dat	0.019561	0.0054456	4.36189	5	0.921	0.464239175	0.051936812	0	0	0.167987345	0.03440046	0	0	
80 seconds.asc	0.009821	0.0025314	1.99724	10	0.933	0.61747303	0	0.062741161	0	6.12E-05	0	-4945.812234	0	
100 seconds.asc	0.0048746	0.000912	0.71957	10	0.811	0.404273028	0	0.151443795	0	0.000274964	0	1598.962712	0	
120 seconds.asc	0.0053657	0.0010087	0.7959	10	0.809	0.421123586	0	0.040361017	0	0.000285276	0	1671.852771	0	
140 seconds.asc	0.0048199	0.0009082	0.7166	10	0.81	0.424654133	0	0.03550843	0	0.000209521	0	1570.121252	0	
160 seconds.asc	0.0055084	0.0010291	0.81195	10	0.807	0.424775619	0	-0.002885476	0	0.000212876	0	1620.165271	0	
180 seconds.asc	0.0054071	0.001052	0.83004	10	0.82	0.419179792	0	-0.010647131	0	0.000168207	0	1525.588836	0	
200 seconds.asc	0.0045912	0.0008512	0.67158	10	0.799	0.406233456	0	0.004930425	0	0.000280181	0	1804.626384	0	
220 seconds.asc	0.0038409	0.0007135	0.56292	10	0.801	0.390064762	0	0.062675638	0	0.000202398	0	1762.003301	0	
240 seconds.asc	0.0127859	0.0052655	4.15447	10	1.109	0.508191831	0	0.152829598	0	0.000179382	0	305.6461249	0	
260 seconds.asc	0.0047939	0.000856	0.67537	10	0.806	0.409065796	0	0.067571024	0	0.016792572	0	-95.1412608	0	
280 seconds.asc	0.0054237	0.0009501	0.74959	10	0.806	0.412687943	0	0.076445173	0	0.023738184	0	-95.14707657	0	
300 seconds.asc	0.006478	0.0011652	0.91934	10	0.803	0.417832598	0	0.052082381	0	0.011309902	0	-95.10755502	0	

Table S2: Fitting data for standards ZIF-8 & Dichlorobis(1-MeIM)zinc(II)

						hexaquazinc2+			Tetrakis(1-MeIM)zinc2+				
Data	rfactor	chinu	chisqr	nv ary	scale by	weight	error	e0	error	weight	error	e0	error
2 seconds.dat	0.0318555	0.010498	8.06249	5	0.79	0.713626556	0.011406277	0	7065.263686	1.42312E-07	0.114675274	0	0.377661871
4 seconds.asc	0.0398551	0.0132073	10.1432	5	0.73	0.730358382	0.012793738	0	7065.263686	3.41093E-09	0.128622223	0	0.377661871
6 seconds.asc	0.0159443	0.0046358	5.06692	5	0.709	0.708816701	0.00933624	0	0.327171167	6.72E-08	0.155177307	0	9941.642394
8 seconds.asc	0.0155452	0.0045996	5.02733	5	0.709	0.708819849	0.009299766	0	0.327171167	2.72E-08	0.154569023	0	9941.642394
10 seconds.asc	0.0158369	0.004642	5.07366	5	0.709	0.708819928	0.009342489	0	0.327171167	2.72E-08	0.155278219	0	9941.642394
12 seconds.asc	0.0567664	0.0192728	9.73275	5	0.722	0.722495472	0.019058317	0	0.741862743	1.99E-08	0.309478375	0	3.853816903
14 seconds.asc	0.0179228	0.0055388	2.90231	10	0.784	0.568433124	0.035436821	0.1098754	0.086189698	7.12E-07	0.162431657	4.250492365	303877.1834
16 seconds.asc	0.0179799	0.0055492	2.90777	10	0.782	0.571075819	0.035280451	0.092187794	0.086253693	3.66E-08	0.156299727	4.172538492	5836242.756
18 seconds.asc	0.0606528	0.0205875	10.39669	5	0.727	0.700817057	0.019697596	0	0.741862743	1.49E-07	0.319857554	0	3.853816903
20 seconds.asc	0.0630022	0.0213053	10.75919	5	0.73	0.689814017	0.020038076	0	0.741862743	3.78E-08	0.325387789	0	3.853816903
22 seconds.asc	0.0619328	0.0212279	10.72009	5	0.73	0.696361895	0.02000162	0	0.741862743	1.92E-06	0.324794147	0	3.853816903
24 seconds.asc	0.0182416	0.0056317	2.95099	10	0.782	0.562393299	0.035844474	0.110077666	0.090975538	7.36E-07	0.173892548	4.1757527	302132.7138
26 seconds.asc	0.0188279	0.0060525	3.17149	10	0.785	0.574165352	0.041531418	0.107241562	0.097290463	1.83E-08	0.18490227	2.993190944	13061144
28 seconds.asc	0.0152077	0.0047935	2.51179	10	0.784	0.588615156	0.033862637	0.157531936	0.075513735	8.18E-08	0.097438987	3.525850083	2505694.377
30 seconds	0.0282043	0.0113234	9.07007	5	0.887	0.727021029	0.012040918	0	0	9.16E-09	0.122750994	0	0
32 seconds	0.0244495	0.0078318	6.27325	5	0.75	0.683666112	0.010013824	0	0	5.60E-08	0.102086162	0	0
34 seconds	0.023157	0.0070049	5.61094	5	0.78	0.570075765	0.009470459	0	0	0.022635171	0.096547427	0	0
36 seconds	0.0208546	0.0082569	6.61381	5	0.942	0.557477063	0.010282031	0	0	0.083580744	0.104820999	0	0
38 seconds	0.0186855	0.007178	5.74958	5	0.961	0.461918145	0.00958674	0	0	0.149236203	0.097732985	0	0
40 seconds	0.0148145	0.006117	4.89972	5	1.007	0.465358432	0.008849905	0	0	0.150357549	0.090221073	0	0
42 seconds	0.01521	0.0071638	5.73818	5	1.094	0.441473593	0.009577244	0	0	0.1764646	0.097635981	0	0
44 seconds	0.0197314	0.0089987	7.20797	5	1.094	0.362494603	0.010733955	0	0	0.215097024	0.109428218	0	0
46 seconds	0.0180073	0.0074402	5.95957	5	1.065	0.289475693	0.009760242	0	0	0.224915789	0.099501647	0	0
48 seconds	0.0155456	0.0059986	4.80491	5	1.034	0.264796631	0.008763874	0	0	0.187606658	0.089346372	0	0
50 seconds	0.0173071	0.0056688	4.54073	5	0.979	0.160774445	0.00851954	0	0	0.223771159	0.086853205	0	0
52 seconds	0.0164976	0.0056443	4.52108	5	0.99	0.17857451	0.008501082	0	0	0.19123575	0.086665023	0	0
54 seconds	0.0186932	0.0062081	4.97272	5	0.977	0.157256572	0.008915591	0	0	0.198196772	0.090890774	0	0
56 seconds	0.0194597	0.0061997	4.966	5	0.972	0.112979271	0.008909563	0	0	0.234014495	0.090829324	0	0
58 seconds	0.0161209	0.0050471	4.04275	5	0.97	0.134859782	0.008038808	0	0	0.222994489	0.081952337	0	0
60 seconds.dat	0.019561	0.0054456	4.36189	5	0.921	0.069400305	0.00835008	0	0	0.219171874	0.08512562	0	0
80 seconds.asc	0.009821	0.0025314	1.99724	10	0.933	0.095708956	0	1.384941257	0	0.220161225	0	0.923271715	0
100 seconds.asc	0.0048746	0.000912	0.71957	10	0.811	0.02714733	0	0.0701229	0	0.340466245	0	1.07133093	0
120 seconds.asc	0.0053657	0.0010087	0.7959	10	0.809	0.030482861	0	0.34732248	0	0.356830785	0	1.112144219	0
140 seconds.asc	0.0048199	0.0009082	0.7166	10	0.81	0.022519459	0	0.630216324	0	0.362800655	0	1.208555004	0
160 seconds.asc	0.0055084	0.0010291	0.81195	10	0.807	0.018128848	0	0.947517568	0	0.364257194	0	1.294450847	0
180 seconds.asc	0.0054071	0.001052	0.83004	10	0.82	0.038309326	0	1.123280527	0	0.362219864	0	1.251034042	0
200 seconds.asc	0.0045912	0.0008512	0.67158	10	0.799	0.041236211	0	1.518816898	0	0.351257852	0	1.322752022	0
220 seconds.asc	0.0038409	0.0007135	0.56292	10	0.801	0.029635097	0	2.183768138	0	0.380930486	0	1.169095039	0
240 seconds.asc	0.0127859	0.0052655	4.15447	10	1.109	0.12143552	0	0.767981141	0	0.479313476	0	0.86058932	0
260 seconds.asc	0.0047939	0.000856	0.67537	10	0.806	0.011223832	0	1.644913105	0	0.364308187	0	1.124120064	0
280 seconds.asc	0.0054237	0.0009501	0.74959	10	0.806	0.009845177	0	1.120854542	0	0.359126962	0	1.090681101	0
300 seconds.asc	0.006478	0.0011652	0.91934	10	0.803	0.014331766	0	0.956263105	0	0.35968395	0	1.085681219	0

Table S3: Fitting data for standards hexaquazinc2+ & Tetrakis(1-MeIM)zinc2+

						ZnO			
Data	rfactor	chinu	chisqr	nv ary	scale by	weight	error	e0	error
2 seconds.dat	0.0318555	0.010498	8.06249	5	0.79	0.030844726	0.041905489	0	0.240014676
4 seconds.asc	0.0398551	0.0132073	10.1432	5	0.73	4.90582E-10	0.047002969	0	0.240014676
6 seconds.asc	0.0159443	0.0046358	5.06692	5	0.709	4.75E-05	0.06012781	0	2.797140348
8 seconds.asc	0.0155452	0.0045996	5.02733	5	0.709	4.59E-05	0.059892026	0	2.797140348
10 seconds.asc	0.0158369	0.004642	5.07366	5	0.709	4.59E-05	0.060166693	0	2.797140348
12 seconds.asc	0.0567664	0.0192728	9.73275	5	0.722	2.38E-08	0.127134417	0	0.31741642
14 seconds.asc	0.0179228	0.0055388	2.90231	10	0.784	0.009462839	0.01315953	-2.659308989	4.894083327
16 seconds.asc	0.0179799	0.0055492	2.90777	10	0.782	0.002289208	0.013397717	-2.623536158	20.36617215
18 seconds.asc	0.0606528	0.0205875	10.39669	5	0.727	0.026136026	0.131398942	0	0.31741642
20 seconds.asc	0.0630022	0.0213053	10.75919	5	0.73	0.040147429	0.133670394	0	0.31741642
22 seconds.asc	0.0619328	0.0212279	10.72009	5	0.73	0.034061179	0.13342696		
24 seconds.asc	0.0182416	0.0056317	2.95099	10	0.782	0.010355308	0.013761858	-2.54949103	4.543668411
26 seconds.asc	0.0188279	0.0060525	3.17149	10	0.785	1.78E-08	0.014126668	-2.397853405	2709203.372
28 seconds.asc	0.0152077	0.0047935	2.51179	10	0.784	6.18E-09	0.010560283	-3.302179854	6939745.911
30 seconds	0.0282043	0.0113234	9.07007	5	0.887	0.043165739	0.045348216	0	0
32 seconds	0.0244495	0.0078318	6.27325	5	0.75	6.58E-09	0.037713846	0	0
34 seconds	0.023157	0.0070049	5.61094	5	0.78	1.25E-05	0.035667563	0	0
36 seconds	0.0208546	0.0082569	6.61381	5	0.942	1.36E-08	0.038724154	0	0
38 seconds	0.0186855	0.007178	5.74958	5	0.961	1.57E-08	0.036105548	0	0
40 seconds	0.0148145	0.006117	4.89972	5	1.007	5.89E-08	0.033330428	0	0
42 seconds	0.01521	0.0071638	5.73818	5	1.094	4.51E-08	0.036069725	0	0
44 seconds	0.0197314	0.0089987	7.20797	5	1.094	4.66E-08	0.040426128	0	0
46 seconds	0.0180073	0.0074402	5.95957	5	1.065	1.03E-05	0.036758942	0	0
48 seconds	0.0155456	0.0059986	4.80491	5	1.034	1.34E-11	0.033007184	0	0
50 seconds	0.0173071	0.0056688	4.54073	5	0.979	3.51E-05	0.032086222	0	0
52 seconds	0.0164976	0.0056443	4.52108	5	0.99	4.34E-06	0.032016702	0	0
54 seconds	0.0186932	0.0062081	4.97272	5	0.977	7.19E-07	0.033577824	0	0
56 seconds	0.0194597	0.0061997	4.966	5	0.972	0.000192754	0.033555122	0	0
58 seconds	0.0161209	0.0050471	4.04275	5	0.97	4.47E-06	0.030275692	0	0
60 seconds.dat	0.019561	0.0054456	4.36189	5	0.921	3.44E-06	0.031447999	0	0
80 seconds.asc	0.009821	0.0025314	1.99724	10	0.933	9.42E-09	0	-1.55E-10	0
100 seconds.asc	0.0048746	0.000912	0.71957	10	0.811	0.038416539	0	-1.55E-10	0
120 seconds.asc	0.0053657	0.0010087	0.7959	10	0.809	5.33E-09	0	-1.55E-10	0
140 seconds.asc	0.0048199	0.0009082	0.7166	10	0.81	1.24E-08	0	-1.55E-10	0
160 seconds.asc	0.0055084	0.0010291	0.81195	10	0.807	2.30E-07	0	-1.55E-10	0
180 seconds.asc	0.0054071	0.001052	0.83004	10	0.82	2.00E-08	0	-1.55E-10	0
200 seconds.asc	0.0045912	0.0008512	0.67158	10	0.799	2.66E-08	0	-1.55E-10	0
220 seconds.asc	0.0038409	0.0007135	0.56292	10	0.801	3.00E-05	0	-1.55E-10	0
240 seconds.asc	0.0127859	0.0052655	4.15447	10	1.109	3.11E-08	0	-1.55E-10	0
260 seconds.asc	0.0047939	0.000856	0.67537	10	0.806	0.005071468	0	-1.55E-10	0
280 seconds.asc	0.0054237	0.0009501	0.74959	10	0.806	0.000437286	0	-1.55E-10	0
300 seconds.asc	0.006478	0.0011652	0.91934	10	0.803	8.83E-06	0	-1.55E-10	0

Table S4: Fitting data for standard ZnO